Derivation of RCM-driven potential evapotranspiration for Great Britain

Science Report/Project Note – SC090016/PN2

Christel Prudhomme, Sue Crooks, Leonore Boelee, Jennifer Williamson and Helen Davies

October 2012

This report is the result of research commissioned and funded by the Environment Agency's Science Programme, the Department for Environment, Food and Rural Affairs, UK Water Industry Research, the Natural Environment Research Council and Wallingford HydroSolutions

Published by:

Centre for Ecology and Hydrology, Maclean Building, Benson Lane, Crowmarsh Gifford, Wallingford, Oxfordshire, OX10 8BB

Tel: +44 (0)1491 838800 Fax: +44 (0)1491 622424
www.ceh.ac.uk

Author(s):
Christel Prudhomme, Sue Crooks, Leonore Boelee, Jennifer Williamson and Helen Davies

Dissemination Status:
Publicly available

Keywords:
Potential evapotranspiration, Penman-Montieth equations, hydrology, climate change

Research Contractor:
Centre for Ecology & Hydrology, Maclean Building, Wallingford, Oxfordshire OX10 8BB
Tel: 01491 692381

Environment Agency's lead:
Glenn Watts

Environment Agency's Project Manager:
Stuart Allen, Science Department, Ipswich

Defra project officer: Mike Walker/Carol Skilling

UKWIR project officer: Owen Bramwell

Collaborator(s):
Wallingford Hydro Solutions
BGS

Science Project Number:
SC090016

Executive summary

Project note on how to derive potential evapotranspiration using different PE methods and climate input variables and implication for hydrological modelling.

Table of contents

Table of figures

Table of tables

Section I Background information

I. 1 Future flows and groundwater levels project

Climate change will increase temperatures and change rainfall across England, Wales and Scotland. In turn, this will modify patterns of river flow and groundwater recharge, affecting the availability of water and changing the aquatic environment. There have been many studies of the impact of climate change on river flows in different parts of the UK, but coverage is uneven and methods vary. This means that it is very difficult to compare between different locations, and hard to identify consistent appropriate adaptation responses.

The project 'Future Flows and Groundwater Levels' will deliver two main products:

(i) national maps (or 'snap shots') of changes in river flow statistics (including mean monthly flows and low flow statistics) for most large rivers of Great Britain for three time horizons: 2020s, 2050s and 2080s;
(ii) daily time series of flows from 1950 to 2100 at 200 river sites and 30 boreholes across Great Britain so that the range of possible changes in both river flow and groundwater levels in the next 100 years can be examined.

These two products provide a complementary assessment of the possible impact of climate on river flows in Great Britain, by focusing on the geographic variability of climatic impact on river flows (national maps) and on the temporal evolution of changes and in particular an assessment of changes in the year-to-year variability (daily time series).

At the end of the project, the daily time series will be made accessible to the whole research community so that further impact analyses can be made on a range of specific areas such as fishery, freshwater ecology, water availability etc… The length (over 150 years) and geographical spread (over Great Britain) of the generated series will enable powerful spatio-temporal analysis of the impact of climate change on UK rivers, for the first time possible at such a scale in Great Britain thanks to a strict methodological framework which will ensure consistency, and hence comparability, of all generated data.

To derive the data, the project will exploit the latest UK Climate Impacts Programme scenarios (Murphy et al., 2009) and will set the range of changes given by the daily time series in the context of the wider climate change uncertainty as defined by the UKCP09 probabilistic products. This means that the same methodology must be used to derive both time series and probabilistic changes, so they can be compared.

I. 2 UKCP09 products

The latest products from the UK Climate Impact Programme (UKCIP) are in the form of probabilistic climate change projections and result from an innovative modelling approach from the Met Office Hadley Centre climate model HadCM3/HadRM3 (Murphy et al., 2009). The approach uses a perturbed physics ensemble (PPE) to generate climate projections of different possible realisations of the future. The method also includes some of the variability introduced when different global climate models (GCM) are used. The complete set of probabilistic projections therefore includes both internal modelling variability (using the PPE) and external modelling variability (from the use of different GCMs), as well as some information on climate variability.

Associated with the UK Climate Projection UKCP09 probabilistic scenarios is the UKCP09 Weather Generator, a stochastic model that produces synthetic daily time series of weather

variables (temperature, rainfall, humidity and sunshine amount) consistent with each other, on a 5-km grid. Many different series can be simulated, all statistically equivalent and matching statistical properties representative of historical observations or including changes suggested by the UKCP09 monthly probabilistic sample. However, the UKCP09 Weather Generator creates time series that are independent for each grid, thus ignoring any spatial consistency, and that are representative of a stationary climate, hence removing any transient progression of climatic change.

Additional UKCP09 by-products are available in the form of daily time series from the Met Office Hadley Centre regional climate model HadRM3 run under the PPE framework. This set only comprises 11 runs each with slightly different model physics, hence accounts for inter-model variability. However, they do not account for as much spread and range in the external variability and climate variability as the probabilistic projections, as they only contain 11 realisations of the climate.

While the HadRM3-PPE time series are available for 62 variables, the UKCP09 probabilistic projections (as a 25-km grid for the UK) only provide change factors for selected variables (Table 1).

Variable	Unit	Change	Temporal averaging	Set
Mean daily temperature	ºC	ºC	Month, season, year	1
Mean daily maximum temperature	ºC	ºC	Month, season, year	1
Mean daily minimum temperature	ºC	ºC	Month, season, year	1
99th percentile of daily maximum temperature	ºC	ºC	Season	1
1st percentile of daily maximum temperature	ºC	ºC	Season	1
99th percentile of daily minimum temperature	ºC	ºC	Season	1
1st percentile of daily minimum temperature	ºC	ºC	Season	1
Precipitation rate	mm/day	%	Month, season, year	1
99th percentile of daily precipitation rate	mm/day	%	Season	1
Relative humidity	%	% (of %)	Month, season, year	1
Total cloud	Fraction	%	Month, season, year	1
Specific humidity	g/kg	%	Month, season, year	2
Net surface long wave flux	W/m^2	W/m^{-2}	Month, season, year	2
Net surface short wave flux	W/m^2	W/m^{-2}	Month, season, year	2
Total downward short wave flux	W/m^2	W/m^{-2}	Month, season, year	2
Mean sea level pressure	hPa	hPa	Month, season, year	2

Table 1: Variables for which UKCP09 probabilistic factor of change scenarios are available - from Murphy et al., 2009; http://ukclimateprojections-ui.defra.gov.uk/ui/req_bldr/data_src.php

The methodology used to generate the gridded probabilistic projections involved two separate independent runs (generating set 1 or set 2) for each grid cell. Because of this independence, it is not possible to use in combination projections from variables of different sets, or from different cells. This considerably restricts the potential use of such factors, e.g. to derive complex variables such as potential evapotranspiration, or to undertake analysis at the national scale.

Probabilistic changes are also provided for large river basins and administrative regions, with one set of variables for each region (hence eliminating the spatial independence issue). However, they have two main disadvantages: (i) by construction, they exclude any spatial variability within the area (as there is only one set of changes for each variable for the whole region); (ii) there is no spatial dependence of the probabilistic changes between different regions.

As a result, the 11-RCM HadRM3-PPE transient daily time series is the only product that can be used consistently throughout the project, to ensure comparability of results of both national and catchment modelling, and to provide information on the possible speed of climatic changes within 150 years. The UKCP09 probabilistic sample will be considered for a few case studies, to identify where the results from the 11-RCM HadRM3-PPE sit within the larger climate change uncertainty.

Section II Concept of evapotranspiration and objectives of this analysis

Water running off into rivers and recharging groundwater aquifers depends on the amount of precipitation that falls on the ground, and the amount of water that does not reach the river: the losses. Accurate estimation of river flows and groundwater levels is only possible with accurate estimation of these losses. The main loss of water is through evapotranspiration, as water is re-distributed back into the atmosphere through evaporation from the land surface and transpiration from vegetation.

Evaporation occurs when water is converted from a liquid state to a vapour state. The rate is controlled by the availability of energy at the evaporating surface, and the ease with which water vapour can diffuse into the atmosphere (Shuttleworth, 1993). Evaporation occurs from all land surfaces while transpiration is loss through the stomata of vegetation. Evaporative losses are determined by atmospheric properties such as humidity, temperature, wind speed and radiation in combination and interaction with plant physiology and availability of water in the soil. Soil water availability depends on antecedent precipitation and evaporation, depth and type of soil and rooting depth of the vegetation. Where soil moisture is not a limiting factor, evaporation is said to take place at the maximum possible rate determined by the atmospheric conditions, called 'potential evapotranspiration' (PE, PET, ET_0, or E_0); where availability of water in the soil is limited, causing plant stress, the real loss of water to the atmosphere is called 'actual evapotranspiration' (AE or ET). Because plants can actually only evaporate the water available to them, AE can vary from zero (when there is no water available) to a maximum equal to PE (when there is enough water in the soil to entirely satisfy the plants' demands). Reference crop evaporation (E_{rc}) is the rate of evaporation of an idealised grass crop, and is also often estimated.

In most catchment-based hydrological models two concepts of evaporative losses are used. One is potential evaporation (PE) which is the maximum possible rate and the other is actual evaporation (AE) which is the loss which actually occurs given the availability of soil moisture to evaporate. The models assume a grass-reference PE, converted to different AE from different vegetation if land use is explicitly accounted for. These concepts are detailed in the next section. Computations of AE are done at regular time steps as a compromise between the continuous physical phenomenon, and the data availability and running time necessary for the computations.

The tools to be used to generate daily time series of river flows and groundwater level in the project are conceptual models requiring three main climate input data time series: precipitation, PE and temperature (for accounting in the snow melt module). Precipitation and temperature are standard outputs from climate models, and are discussed in different project notes. PE, however, is not always available directly from climate models, and must be derived using information available from the climate model outputs. For the generated river flow and groundwater level time series to be set in the context of the probabilistic projections, the same methodology must be used to derive PE throughout the project, by using climate variables available from both HadRM3-PPE runs and UKCP09 probabilistic change factors.

In addition, the modelling tools that are to be used in the project to derive the daily river flow and groundwater level time series have been calibrated using specific PE estimates. For the model errors to remain of the same order of magnitude as when using the original PE estimates (and thus the simulated series to be as realistic as possible), the method used to calculate PE for the whole project must generate estimates as close as possible to those used for the model calibration, and in particular to be able to reproduce well seasonal and inter-annual variability, and spatial patterns of PE magnitude. While it is expected that no simplified method can achieve an exact match with sophisticated PE estimates, this note

investigates the magnitude of errors propagated to the river flow using different PE estimates calculated from observed data and calculated from RCM-derived time series.

The main criteria for the selection of the method to be used in the project to calculate PE are:

- Good reproduction of known PE spatial and temporal variability throughout the UK when PE is estimated using observed variables;
- Good reproduction of known PE spatial and temporal variability throughout the UK when PE is estimated using RCM-driven variables;
- Minimisation of errors in river flow and groundwater level characteristics for the baseline period from PE estimated using both observed and RCM-driven variables.

Section III briefly summarises the concepts of PE and AE, and presents some of the most commonly used methods and associated equations to estimate PE from different climate variables. Section IV presents national GB estimates obtained from all considered methods, using both observed and RCM-driven variables. Section V presents the river flow and groundwater level time series generated using different PE estimates, and discusses the associated errors. Section VI concludes on the project method to estimate PE.

Section III Potential evapotranspiration methods

III. 1 Introduction

By definition PE is a theoretical concept and cannot be measured directly; formulations to estimate PE from measurable climate variables have been researched by hydrologists and agronomists since the early 1900s. Xu & Singh (1998) analysed the dependency of evaporation on meteorological variables at different time scales, and concluded that vapour pressure deficit is a controlling factor of PE for all tested time steps (hourly to seasonal) while wind speed primarily matters at the hourly time step. The importance of temperature and relative humidity decreases with time-aggregation, while radiation shows good relationships with evaporation at all time scales. This suggests that for this project formulations based on temperature, radiation or relative humidity are likely to be preferable to those based on wind speed when estimates are made at daily to monthly time step.

This section provides a list of the most useful concepts and equations which have been used to estimate PE. For example, some formula aim to incorporate two different physical processes of evaporation, one driven by the plants (mainly driven by the photosynthesis process) and one driven by the atmosphere (e.g. due to the wind); they are usually referred to a 'combined' equations. Other formula consider evaporation processes as a whole and main driven by plants and use a few climate variables as proxy for both plants and atmosphere evaporation (e.g. radiation as main energy source for photosynthesis, or 'radiation-driven' equations; or temperature as strongly correlated with radiation, or 'temperature-driven equations). Because different authors suggest different approximations of complex physical formulations, the source and units of the given equations are systematically provided. Note that alternative formulations can be found in the literature, and could result in different estimates.

III. 2 Units for potential evapotranspiration

Depending on the family (e.g. 'combined', 'radiation-driven', 'temperature-driven') to which the PE method belongs, PE is either calculated in terms of energy, mainly in MJ m^{-2} day^{-1}, or as a water depth, in mm day^{-1}. Using the latent heat of vaporization of water, both units are linked by:

$$PE[mm\ day^{-1}] = \frac{1}{\rho_w \lambda} PE[MJ\ \ m^{-2}\ day^{-1}]$$

with ρ_w, density of water ≈1000 [kg m^{-3}] and λ latent heat of vaporisation [MJ kg^{-1}]. A formulation for λ is given in the next section.

III. 3 UK reference PE

III. 3. 1. UK Met Office MORECS

The UK Met Office derived a set of monthly PE in 1981 using the Meteorological Office Rainfall and Evaporation Calculation System (MORECS, Thompson et al. (1982)). The system was modified in the 1990s (Hough et al., 1997) and is the standard PE used in many hydrological models in the UK. MORECS was designed to provide estimates of weekly and monthly evaporation and soil moisture deficit in the form of averages over a 40-km grid across Great Britain. Daily PE was estimated for each grid square for a range of surface covers from bare soil to forest using a modified form of the Penman-Monteith combination

equation. Calculations are done separately for day and night time periods and then combined to provide the weekly and monthly time series.

The monthly MORECS PE estimates were used to calibrate the hydrological models CLASSIC and PDM and the conceptual groundwater level model used in this project. These national PE estimates were preferred to any local computations as they provide a national estimation consistent in space and time that would be difficult to achieve otherwise due to data availability limitations.

III. 3. 2. **UK Met Office offline MOSES**

MOSES (Met Office Surface Exchange Scheme) was developed during the 1990s for use in weather forecast and climate models (Cox et al., 1999), and uses the Penman-Monteith approach. Initially coupled within the Met Office land surface models MOSES data is available in two versions. Online MOSES data is driven by radar rainfall and remotely sensed inputs, and is available hourly on a 2km grid in real time through the Numerical Weather Prediction UK Post Processing output. There is about three and a half years of PE data available in this archive calculated with the same version number. Offline MOSES data is driven by MORECS climate station meteorological data, is available on the MORECS 40km grid squares, at a daily time step from 1961. This provides a consistent long term dataset which can be used to calibrate rainfall runoff models for water resource purposes. Hough (2003) details the assumptions applied to the daily MORECS meteorological station data to run it through the hourly offline MOSES model.

There are structural differences between MOSES and MORECS (Hough, 2003): (i) online MOSES spatial resolution is 5-km (now 2-km) while MORECS is 40-km; (ii) the canopy resistance to moisture flow has fixed values in MORECS but is interactive in online and offline MOSES; (iii) time step of calculation is hourly for online and offline MOSES and daily for MORECS; (iv) number of surface types is 15 for MORECS, including many seasonal crops, but only 7 for online MOSES (1 in offline MOSES); (v) MOSES uses soil data for the whole of the UK while MORECS only uses data for England and Wales, and extrapolates the information for Scotland.

Offline MOSES PE was aggregated to monthly periods. This v2.0 offline data was used to originally calibrate the hydrological model CERF.

III. 4 Physical equations of the soil-plant-atmosphere system

While PE formulations have been summarised by sets of equations of varying complexity, requiring more or less climate variables as input, most depend on intermediate variables reflecting the different physical processes occurring in the evaporation processes. The most useful equations to estimate these intermediate variables are provided in this section. They summarise some of the water properties and other controlling characteristics of the soil-plant-atmosphere system.

III. 4. 3. **Solar declination**

The solar declination δ is the angle between the rays of the Sun and the plane of the Earth's equator. It depends on the time of the year and is given by Shuttleworth (1993) [eq. 4.4.3]:

$$\delta\ [radians] = 0.4093 \sin\left(\frac{2\pi}{365} J - 1.405\right)$$

with J Julian day number (or number of the day in the year).

III. 4. 4. **Relative distance between the Earth and the Sun**

Because the Earth orbits around the Sun following an ellipse and not a circle, the distance between Earth and Sun varies throughout the year. This relative Earth-Sun distance takes as its reference distance that for an equinox day, when the tilt of the Earth and the direction of the Sun are perpendicular, and is given by Shuttleworth (1993) [eq. 4.4.5]:

$$d_r = 1 + 0.033\ cos\left(\frac{2\pi}{365}J\right)$$

with J Julian day number (or number of the day in the year).

III. 4. 5. **Sunset hour angle**

The sunset hour angle ω_s is the angle by which the rays of the Sun reach the Earth's surface. It depends on latitude and time of the year and is given by Shuttleworth (1993) [eq. 4.4.2]:

$$\omega_s[radians] = \arccos\left(-tan\Phi\ tan\delta\right)$$

with Φ latitude [radians] (positive for North hemisphere, negative for South) and δ solar declination [radians].

III. 4. 6. **Maximum possible daylight length**

The maximum possible daylight hours N, is the length of the period when the rays of the Sun reach the Earth's surface. It depends on the sunset hour angle and is given by Shuttleworth (1993) [eq. 4.4.1]::

$$N = \frac{24}{\pi}\omega_s$$

with ω_s sunset hour angle [radians]

III. 4. 7. **Saturated water vapour pressure**

The air is said to be saturated when rates of vaporisation and condensation are equal and there is no evaporation possible (i.e. the air cannot contain more water vapour without condensation). At a given temperature this equilibrium occurs for a particular vapour pressure e_s, called the saturated vapour pressure and given by Shuttleworth (1993) [eq. 4.2.2]:

$$e_s[kPa] = 0.6108\ exp\left(\frac{17.27\ T}{237.3 + T}\right)$$

with T air temperature [ºC].

III. 4. 8. **Actual water vapour pressure**

The actual water vapour pressure represents the amount of water contained in the air at dew point temperature. It is given by Allen et al. (1998) [eq. 14 p 37]:

$$e_d[kPa] = 0.6108\ exp\left(\frac{17.27\ T_d}{237.3 + T_d}\right)$$

with T_d dew point temperature [ºC].

III. 4. 9. Gradient of vapour pressure curve

Vapour pressure is the pressure of a vapour at equilibrium with its condensed phase, and depends on temperature. The gradient of the vapour pressure curve Δ is the slope of the nonlinear pressure-temperature relationship, and is thus temperature-dependant. It is given by Shuttleworth (1993) [eq. 4.2.3]:

$$\Delta[kPa°\mathrm{C}^{-1}] = \frac{4098\, e_s}{(237.3 + T)^2}$$

with e_s saturated vapour pressure [kPa] and T air temperature [ºC].

III. 4. 10. Latent heat of vaporisation

Latent heat of vaporisation λ is the amount of energy that is needed for water to be transformed from a liquid into a gaseous state. It is virtually unchanged with atmospheric pressure but does change with temperature (Jensen et al., 1990). It is given by Shuttleworth (1993) [eq. 4.2.1]:

$$\lambda[MJ\ kg^{-1}] = 2.501 - 0.002361T$$

with T air temperature [ºC]. Assuming T_s to be equal to 20ºC, λ is often approximated to 2.45 MJ kg^{-1}.

III. 4. 11. Atmospheric pressure

The pressure of the atmosphere P changes with altitude, as it relates to the weight of the air above and is given by Allen et al. (1998) [eq. 7, p31]:

$$P[kPa] = 101.3\left(\frac{293 - 0.0065z}{293}\right)^{5.26}$$

with z elevation above sea level [m].

III. 4. 12. Absolute humidity or water vapour density

The absolute humidity ρ is the water vapour density, i.e. the mass of water vapour per unit volume of moist air (Jensen et al., 1990). It can be calculated from the ideal gas law and is given by Jensen et al. (1990) [eq. 7.7 and 7.8b]:

$$\rho[kg\ m^{-3}] = 3.483\frac{P - 0.378e_d}{T}$$

with P vapour pressure [kPa], T temperature [ºK] and e_d actual water vapour pressure [kPa]

III. 4. 13. Relative humidity and vapour pressure

Relative humidity RH is the amount of water air can hold at a certain temperature, i.e. the percentage ratio of the actual to the saturation vapour pressure (Linsley et al., 1988). It is therefore also the ratio of the amount of moisture in a given space to the amount the space could contain if saturated. It is linked to the actual vapour pressure by Jensen et al. (1990) [eq. 2.7]:

$$RH = 100\frac{e_d}{e_s}$$

with e_s saturated vapour pressure [kPa] and e_d actual vapour pressure [kPa].

This relationship is also often used to estimate actual vapour pressure from relative humidity.

III. 4. 14. **Cloudiness factor**

Clouds are important as they have two radiative effects: they reflect a large proportion of incident sunlight back up into space from their top, and they efficiently emit thermal radiation down to the Earth's surface. The cloudiness factor f expresses how much cloud cover there is in the atmosphere, and is directly related to the number of bright sunshine hours within a day. It is given by Shuttleworth (1993) [eq. 4.2.12]:

$$f = \left(a_c \frac{b_s}{a_s + b_s}\right)\frac{n}{N} + \left(b_c + \frac{a_s}{a_s + b_s}a_c\right)$$

with n the bright sunshine hours [h], N maximum possible daylight hours [h], a_s the fraction of extraterrestrial radiation S_0 entering the atmosphere on an overcast day (when $n = 0$), $a_s + b_s$ the fraction of extraterrestrial radiation S_0 entering the atmosphere on clear days (they are also known as the Angstrom coefficients) and a_c and b_c the long-wave coefficients for clear skies (with $a_c + b_c = 1$).

The recommended values of the Angstrom coefficients for average climates, when no actual solar radiation data are available are (Shuttleworth, 1993) [p. 4.7]:

$a_s = 0.25$ and $b_s = 0.50$

The indicative values recommended for long-wave coefficients are (Shuttleworth, 1993) [p 4.8] (see also Jensen et al. (1990)) [Table 3.3 p 36]:

$a_c = 1.35$ and $b_c = -0.35$ for arid areas

$a_c = 1.00$ and $b_c = 0.00$ for humid areas

The cloudiness factor calculated in the FAO56 reference Penman-Monteith equation to derive long-wave radiation assumes the values for arid areas. (This is also the formulation suggested by Allen et al. (1998) [eq 39 p 52]).

Taking the long-wave coefficients for arid areas, the cloudiness factor becomes:

$$f = 0.9\frac{n}{N} + 0.1$$

with n the bright sunshine hours [h] and N maximum possible daylight hours [h]

An equivalent expression of the cloudiness factor, which reflects the effect of clouds on short-wave global solar radiation, is given by Jensen et al. (1990) [eq. 3.13]

$$f = a_c \frac{R_s}{S_0} + b_c$$

with R_s solar (short-wave) radiation [MJ m^{-2} day^{-1}] and S_0 extraterrestrial radiation.

III. 4. 15. **Soil heat flux**

The soil heat flux G is the energy that moves from the surface into subsurface soil by conduction. G can be estimated using a heat balance of the soil profile, and depends on soil temperature fluctuations. Its monthly formulation is given by Shuttleworth (1993) [eq. 4.2.18]:

$$G = 0.38\left(T_{day2} - T_{day1}\right)$$

with T_{dayx} mean temperature of day x, and $day2$ separated by one month from $day1$.

Since the magnitude of daily soil heat flux over 10-30 day periods beneath densely planted grass is relatively small, it may be neglected Allen et al. (1994) [eq. 1.59] and thus in the rest:

$$G = 0$$

III. 4. 16. **Psychrometric constant**

The physical and thermodynamic properties of gas-vapour mixtures are described through psychrometry. For water, the psychometric chart describes the thermodynamic properties of moist air at a constant pressure. The psychrometric constant γ relates the partial pressure of water in the air to the air temperature, and is given by Shuttleworth (1993) [eq. 4.2.28]:

$$\gamma[kPa°\mathrm{C}^{-1}] = \frac{c_p P}{\epsilon\lambda}$$

with c_p specific heat of moist air ≈1.1013 [kJ kg^{-1} ºC^{-1}] P atmospheric pressure ≈ 101.3 [kPa], ϵ ratio of molecular weight of water vapour to that for dry air = 0.622 and λ latent heat of vaporisation [MJ kg^{-1}].

III. 4. 17. **Extraterrestrial [solar] radiation**

The extraterrestrial radiation S_0 is the amount of solar energy that reaches the top of the atmosphere. It depends on the angle of radiation from the Sun (declination) and on the length of the day, and thus the latitude and the time of the year. It is given by Shuttleworth (1993) [eq. 4.4.4] (in mm day^{-1}) and Allen et al. (1994) [eq. 1.22], in MJ day^{-1}:

$$S_0[MJ\ m^{-2}\ day^{-1}] = 37.62\ d_r\ (\omega_s sin\Phi sin\delta + cos\Phi cos\delta sin\omega_s)$$

with all variables and units defined as above.

III. 4. 18. **Solar [short-wave] radiation or global radiation or incident solar radiation**

Solar radiation R_s is the amount of energy measured at the Earth's surface including both direct and diffuse short-wave radiation. It is also referred to as global radiation or incident solar radiation (Jensen et al., 1990). It is thus the part of the extraterrestrial short-wave radiation which is not absorbed or reemitted by the clouds. It does not, however, consider the reflected radiation from the Earth's surface. Many different authors suggest different combinations, but the generalised form is recommended by Jensen et al. (1990) [eq. 3.3b]:

$$R_s[MJ\ m^{-2}day^{-1}] = S_0\left(0.25 + 0.50\frac{n}{N}\right)$$

with S_0 extraterrestrial radiation [MJ m^{-2} day^{-1}], N maximum possible daylight hours [h] and n bright sunshine hours [h].

III. 4. 19. **Net solar [short-wave] radiation**

The net solar short wave radiation R_{ns} is the proportion of incident short wave radiation captured at the ground taking into account losses due to reflection. It is given by Shuttleworth (1993) [eq. 4.2.5]:

$$R_{ns}[MJ\ m^{-2}day^{-1}] = (1-\alpha)R_s$$

with α albedo ≈ 0.23 for grass and agricultural crop and R_s incident short wave radiation [MJ m^{-2} day^{-1}]

III. 4. 20. **Net emissivity**

The net emissivity ϵ' is the proportion of radiation reflected by the Earth's surface and takes the general form of Brunt (1934) [eq 14 p122]:

$$\epsilon'[kPa] = a + b\sqrt{e_d}$$

With e_d actual vapour pressure [kPa].

Experimental values for the net emissivity coefficients *a* and *b* are provided by Jensen et al. (1990) [table 3.3, p36]. When used to estimate long-wave radiation, the recommended formulation for average values is Jensen et al. (1990) [eq. 3.18 p36], also found in Shuttleworth (1993) and Allen et al. (1998):

$$\epsilon'[kPa] = 0.34 - 0.139\sqrt{e_d}$$

With e_d actual vapour pressure [kPa].

Idso and Jackson presented a generalised equation for effective emittance based only on air temperature at screen height. With emittance of the ground and crop surface of 0.98, the net emissivity using the Idso-Jackson equation becomes (Jensen et al., 1990) [eq. 3.20 p37],

$$\epsilon'[kPa] = -0.02 + 0.261exp(-7.7\times10^{-4}T^2)$$

with T air temperature [ºC].

III. 4. 21. **Long-wave radiation**

Long-wave radiation is also called thermal radiation. It is the part of the extraterrestrial radiation which is reemitted by the Earth's surface and the clouds. It is thus dependant on the cloud cover, but also on the reflection (or emittance) property of the Earth's surface and of the atmosphere. The net outgoing long wave radiation R_{nl} is thus the amount of energy leaving the earth. The Doorenbos and Pruitt equation below is given by Jensen et al. (1990) [eq. 3.18]:

$$R_{nl}[MJ\ m^{-2}\ day^{-1}] = -f\epsilon'\sigma T^4$$

with *f* cloudiness factor, ϵ' the net emissivity between the atmosphere and the ground [kPa], σ Stefan-Boltzmann constant ≈ 4.903 10^{-9} [MJ m^{-2} day^{-1} K^{-4}] and T mean air temperature [ºK].

III. 4. 22. **Net radiation**

Net radiation R_n is the net input of radiation at the surface, i.e the difference between incoming radiation (from the Sun through the atmosphere) and reflected solar radiation (in the form of short-wave radiation), plus the difference between the incoming long-wave radiation and outgoing long-wave radiation (Shuttleworth, 1993) [eq. 4.2.13], hence:

$$R_n = R_{ns} + R_{nl}$$

By convention, net shortwave (downward) radiation R_{ns} is positive, while net longwave (upward) radiation R_{nl} is negative.

Net radiation can be measured, but such measures are not widely available. Therefore, the equations given above for long-wave and short-wave radiation can be combined to give the following equation to estimate daily R_n (in MJ m^{-2} day^{-1}) from sunshine hours, temperature and vapour pressure (Shuttleworth, 1993) [eq. 4.2.14 corrected]:

$$R_n[MJ\ m^{-2}\ day^{-1}] = (1-\alpha)\left(0.25 + 0.5\frac{n}{N}\right)S_0 - \left(0.9\frac{n}{N} + 0.1\right)\left(0.34 - 0.14\sqrt{e_d}\right)\sigma T^4$$

with α albedo [0.23 for short grass], n bright sunshine hours per day [h], N daily total daylight [h], S_0 extraterrestrial radiation [MJ m^{-2} day^{-1}], e_d actual vapour pressure kPa], σ Stefan-Boltzmann constant ≈ 4.903 10^{-9} [MJ m^{-2} ºK^{-4} day^{-1}] and T mean air temperature [ºK]. Note this equation is stated as being for general purposes (Shuttleworth, 1993) but the values for the coefficients are those derived for southern USA (or arid areas).

III. 5 Combined equations

Penman was the first to derive an equation which combines the energy required to sustain evaporation and an empirical description of the diffusion mechanism by which energy is removed from the surface as water vapour (Shuttleworth, 1993). This has become known as a combination equation. Different versions of the combined equation can be found in the literature. We provide here some of the most commonly used world-wide, and in the UK.

III. 5. 1. **FAO-24 Penman equation**

The FAO-24 Penman equation (Doorenbos & Pruitt, 1977) refers to short grass. The Jensen et al. (1990) formulation is given here [eq. 6.31 & 6.32].

$$PE[mm\ day^{-1}] = c\left[\frac{\Delta}{\Delta+\gamma}(R_n - G) + \frac{\gamma}{\Delta+\gamma}2.7(1 + 0.864U_2)(e_s - e_d)\right]$$

With c adjustment factor = 1, R_n net radiation at crop surface [mm day^{-1}], G soil heat flux = 0 [MJ m^{-2} day^{-1}], Δ gradient of vapour pressure curve [kPaºC^{-1}], γ psychrometric constant [kPaºC^{-1}], U_2 windspeed measured at 2m height [m s^{-1}], $(e_s - e_d)$ vapour pressure deficit [kPa].

This formulation was found to frequently overestimate PE (Allen et al., 1994), mainly because of the procedures used to compute parameters within the equation and partly from the reliability and processing of data. Note that the adjustment factor are likely to be for open water evaporation rather than crop evapotranspiration. First tests showed FAO-24 PE was systematically greater than any other PE in Great Britain. Consequently, estimations using this equation are not discussed further in this document.

III. 5. 2. **FAO-56 reference Penman-Monteith equation**

The FAO-56 reference [crop] Penman Monteith equation was developed by Allen et al. (1998), Allen et al. (1994) to overcome the limitations of FAO-24 Penman. It is given by Allen et al. (1998) [eq. 6 p 24]:

$$PE[mm\ day^{-1}] = \frac{\lambda^{-1}\Delta(R_n - G) + \gamma \frac{900}{T+273}\ U_2(e_s - e_d)}{\Delta + \gamma(1 + 0.34U_2)}$$

with λ latent heat of vaporisation [MJ kg^{-1}], R_n net radiation at crop surface [MJ m^{-2} day^{-1}], G soil heat flux [=0 MJ m^{-2} day^{-1}], T average temperature at 2m height [ºC], U_2 windspeed measured at 2m height [m s^{-1}], $(e_s - e_d)$ vapour pressure deficit for measurement at 2m height [kPa], Δ gradient of vapour pressure curve [kPaºC^{-1}], γ psychrometric constant [kPaºC^{-1}], 900 coefficient for the reference crop in [kJ^{-1} kg ºKday^{-1}], 0.34 coefficient for the reference crop [s m^{-1}]

III. 5. 3. **Modified Penman-Monteith equation**

A modification of the Penman-Monteith equations was suggested for use with the HadRM3 model outputs (Kay et al., 2003) in order to emulate MORECS implementation and is given by [eq. 2.18]:

$$PE[mm\ day^{-1}] = \frac{1}{\lambda}\frac{\Delta(R_n - G) + \rho C_p(e_s - e)/r_a}{\Delta + \gamma(1 + r_s/r_a)}$$

With λ latent heat of vaporisation [= 2.465 MJ kg^{-1}], R_n net radiation at crop surface [MJ m^{-2} day^{-1}], G soil heat flux [=0 Wm^{-2}], $(e_s - e)$ vapour pressure deficit for measurement at 2m height [mb = 1/10kPa], e screen vapour pressure [mb], Δ gradient of vapour pressure curve [mbºC^{-1} = 1/10 kPaºC^{-1}], γ psychrometric constant [=0.066 kPaºC^{-1}], ρ air density [kg m^{-3}], C_p specific heat of air at constant pressure [= 0.001013 MJ kg^{-1}], r_s bulk surface (canopy) resistance [s m^{-1}], r_a bulk aerodynamic resistance [s m^{-1}]

Where

$$\Delta[mb^{\circ}C^{-1}] = \alpha\frac{exp\left(\frac{17.269T}{237.3+T}\right)}{(T+237.3)^2}$$

With α=25040 and T average temperature at 2m height [ºC]

$$e_s[kPa] = 0.611\ exp\left(\frac{19.626\ T}{237.3+T}\right)$$

with T air temperature [ºC]. Note this equation is different from that of III.3.5.

$$e[kPa] = \frac{RH \times e_s}{100}$$

With RH relative humidity [%]

$$r_a = \frac{6.25}{U(10+d)} ln\left(\frac{10}{z_0}\right) ln\left(\frac{6}{z_0}\right) = \frac{243.489}{U(10+d)}$$ [for grass]

With $U(10+d)$ windspeed [m s^{-1}] at reference level (10+d) m above ground, d zero-plane displacement height [0.6 * h = 0.09 m for grass] and z_0 roughness length [0.1h = 0.015 m]

$$\frac{1}{r_s} = \frac{1 - 0.7^L}{r_{sc}} + \frac{0.7^L}{r_{ss}}$$

With r_{sc} surface resistance of the crop freely supplied with water [= 80 (Jan, Feb), 60 (Mar), 50 (Apr), 40(May), 60 (Jun Jul), 40 (Aug, Sep, Oct) and 80 (Nov, Dec)]; r_{ss} surface resistance of bare soil when wet [= 100 sm^{-1}]; L leaf area index [= 2 (Jan, Feb), 3 (Mar), 4 (Apr), 5 (May, Jun, Jul, Aug), 4 (Sep), 3 (Oct), 2.5 (Nov), 2 (Dec). These are MORECS values.

III. 6 Radiation-based formulations

As the first term of the combination equations frequently exceeds the second by a factor of about four, this suggests it is possible to derive a simpler empirical relation between evaporation and radiation (Shuttleworth, 1993). The radiation-based formulations exploit this approximation.

III. 6. 1. Priestley Taylor equation

Priestley and Taylor proposed a simplified version of the combination equation where the aerodynamic component was deleted and the energy component was multiplied by a coefficient $\propto$. It is given by Priestley and Taylor (1972) [eq. 14]:

$$PE[mm\ day^{-1}] = \propto \frac{1}{\lambda} \frac{\Delta}{\Delta + \gamma} (R_n - G)$$

with R_n net radiation [MJ m^{-2} day^{-1}], Δ gradient of vapour pressure curve [kPaºC^{-1}], γ psychrometric constant [kPaºC^{-1}], $\propto$ ≈ 1.26 for relative humidity > 60% (Shuttleworth, 1993 [eq. 4.2.39] and λ latent heat of vaporisation [MJ kg^{-1}]. [Note that $\propto$ is different from α, albedo].

III. 6. 2. Turc equations

In humid climates, the Turc equations (Turc, 1961) have been shown to perform well (Shuttleworth, 1993). The formulation given here is that from Shuttleworth (1993) [eq. 4.2.40 and 4.2.41]:

$$\begin{cases} PE[mm\ day^{-1}] = 0.31\ \dfrac{T}{T+15}(R_{sn} + 2.09)\left(1 + \dfrac{50 - RH}{70}\right) & for\ RH < 50\% \\ PE[mm\ day^{-1}] = 0.31\ \dfrac{T}{T+15}(R_{sn} + 2.09) & for\ RH > 50\% \end{cases}$$

with T average temperature [ºC], R_{sn} net solar radiation (short-wave) [mm day^{-1}] and RH relative humidity [%]

III. 6. 3. Jensen-Haise equation

The Jensen-Haise method was derived from well watered alfalfa in western USA (Jensen and Haise, 1963). The equation given here is that from Jensen et al. (1990) [eq. 6.40]:

$$PE[mm\ day^{-1}] = \frac{1}{\lambda} 0.025(T + 3) R_s$$

with T temperature [ºC] and R_s solar radiation [MJ m^{-2} day^{-1}]

III. 6. 4. **Makkink equation**

The Makkink equation was developed empirically and is commonly used in the Netherlands (Jacobs et al., 2009). Its original general form is given by:

$$PE[mm\ day^{-1}] = \frac{1}{\lambda} c_1 \frac{\Delta}{\Delta + \gamma} R_s + c_2$$

With λ latent heat of vaporisation [MJ kg^{-1}], Δ gradient of vapour pressure curve [kPa^{o}C^{-1}], γ psychrometric constant [kPa^{o}C^{-1}], R_s global radiation [MJ m^{-2} day^{-1}], and c_1 and c_2 empirical constants.

A widely used simplified formula has been derived by de Bruin, determined for the Netherlands (Jacobs et al., 2009) [eq. 3], and is given here in water depth units:

$$PE[mm\ day^{-1}] = \frac{1}{\lambda} \frac{R_n}{R_s} \frac{\Delta}{\Delta + \gamma} R_s$$

with $\frac{R_n}{R_s}$ ratio of net shortwave to global incoming radiation ≈ 0.65 for short grass (hence removing the need for R_n), λ latent heat of vaporisation [MJ kg^{-1}], Δ gradient of vapour pressure curve [kPa^{o}C^{-1}], γ psychrometric constant [kPa^{o}C^{-1}], R_s global (solar) radiation [MJ m^{-2} day^{-1}].

III. 6. 5. **Priestley Taylor with Idso-Jackson simplification**

Idso-Jackson suggested a simplification to estimate net emittance based on air temperature instead of vapour pressure (Shuttleworth, 1993) [eq. 4.2.9, p4.7]. In this context, the Priestley-Taylor – Idso-Jackson PE is given by:

$$\begin{aligned} PE[mm\ day^{-1}] = & \\ & \propto \frac{1}{\lambda} \frac{\Delta}{\Delta + \gamma} (1 - \alpha) \left(0.25 + 0.5 \frac{n}{N}\right) S_0 \\ & - \left(0.9 \frac{n}{N} + 0.1\right) \left(-0.02 + 0.261 exp(-7.7 \times 10^{-4} T^2)\right) \sigma T^4 \end{aligned}$$

with α albedo [0.23 for short grass], n bright sunshine hours per day [h], N daily total daylight [h], S_0 extraterrestrial radiation [MJ m^{-2} day^{-1}], σ Stefan-Boltzmann constant ≈ 4.903 10^{-9} [MJ m^{-2} ^{o}K^{-4} day^{-1}], T mean air temperature [^{o}K], Δ gradient of vapour pressure curve [kPa^{o}C^{-1}], γ psychrometric constant [kPa^{o}C^{-1}], $\propto$ ≈ 1.26 for relative humidity > 60% (Shuttleworth, 1993 [eq. 4.2.39] and λ latent heat of vaporisation [MJ kg^{-1}]. Note this equation is stated as being for general purposes (Shuttleworth, 1993) but the values for the coefficients are those derived for southern USA (or arid areas). [Note that $\propto$ is different from α, albedo].

III. 7 Temperature-based formulations

The physical basis for estimating evaporation using temperature alone is that both terms of the combination equation (energy required to sustain evaporation, and energy removed from the surface as water vapour) are likely to have some relationship with temperature (Shuttleworth, 1993). As the first term is generally greater than the second, correlation between radiation and temperature is used. Note that as extraterrestrial radiation is used in some formula, some authors classify those formula as radiation based. This is not done here as the influence of cloud on radiation is not included.

III. 7. 1. **Hamon equation**

The Hamon equation aimed to formulate a functional relationship between PE and temperature and day-time hours (Hamon, 1961). It was established for the USA and is given by:

$$PE[inches\ day^{-1}] = 0.55\left(\frac{N}{12}\right)^2 \rho_s$$

with N maximum possible daylight hours [h] and ρ_s saturated vapour density [g m^{-3}]

The approximation suggested by Oudin et al. (2005) is given here:

$$PE[mm\ day^{-1}] = \left(\frac{N}{12}\right)^2 exp\left(\frac{T}{16}\right)$$

with T average temperature [ºC] and N maximum possible daylight hours [h]

III. 7. 2. **McGuinness-Bordne equation**

The McGuinness-Bordne equation was developed in the USA. The version described by Oudin et al. (2005) is given here:

$$PE[mm\ day^{-1}] = \frac{1}{\lambda} S_0 \left(\frac{T+5}{68}\right)$$

with λ latent heat of vaporisation [MJ kg^{-1}], T temperature [ºC] and S_0 extraterrestrial radiation [MJ m^{-2} day^{-1}]

III. 7. 3. **Oudin**

Following a review of various PE methods for use as input to hydrological models, Oudin et al. (2005) derived a new temperature-based equation calibrated on catchments in Australia, USA and France. It is given by:

$$\begin{cases} PE[mm\ day^{-1}] = \frac{1}{\lambda} S_0 \left(\frac{T+5}{100}\right) & if\ T > -5℃ \\ PE[mm\ day^{-1}] = 0 & if\ T \leq -5℃ \end{cases}$$

with λ latent heat of vaporisation [MJ kg^{-1}], T temperature [ºC] and S_0 extraterrestrial radiation [MJ m^{-2} day^{-1}]

III. 7. 4. **Blaney-Criddle equations**

The Blaney-Criddle equations were derived to estimate the irrigation requirements of crops in Western USA (Blaney and Criddle, 1950). Its general form is, for a given month:

$$PE = kTp_d$$

with

$$p_d = 100\frac{N_d}{\sum_{i=1}^{365} N_i}$$

with, p_d mean daily percent of annual daytime hours for day d, T mean air temperature and k monthly consumptive use coefficient. The coefficients k depend on crop, location and season, hence it is recommended to calibrate to the area of interest for each month.

Alternatives, such as the FAO-24 BC (Doorenbos and Pruitt, 1977) are also currently found in the literature (e.g. Jensen et al. (1990) [eq.6.52 to 6.55]) of the general form:

$$PE = a + kp_d(0.46T + 8.13)$$

with the same notations as above.

Two sets of model parameters have been fitted to the above equation for this project, to the MORECS and offline MOSES mean monthly gridded PE, and have been considered as possible PE formulation for the project. Table 2 presents the monthly parameter sets with the associated explained variance (R^2), with the higher R^2, the more variance is explained. Maximum R^2 is 1 and values above 0.6 are considered acceptable. Note that in winter PE is not well reproduced by the equations probably because T and p_d are not a good proxy for radiation. Note that however, for hydrological processes, PE is low in winter months and has a much smaller influence over runoff than precipitation. Poor reproduction of winter PE is hence not considered as a strong limitation for this project.

	MORECS			Offline MOSES		
	a	k	R^2	a	k	R^2
January	-0.0556	0.3129	0.3895	-0.2651	0.258	0.2576
February	-0.3354	0.4571	0.6425	-0.8797	0.5909	0.7108
March	-0.6516	0.6439	0.6574	-1.3742	0.7983	0.8133
April	-2.2882	1.1354	0.7963	-2.883	1.2437	0.7585
May	-4.7247	1.6087	0.7470	-4.0531	1.4091	0.6280
June	-6.8267	1.7882	0.6635	-5.5014	1.5513	0.4830
July	-8.0714	1.9678	0.8124	-7.2294	1.813	0.6885
August	-5.7814	1.6632	0.8939	-6.2159	1.729	0.8541
September	-1.9942	0.9488	0.8003	-3.2903	1.2057	0.891
October	-0.4061	0.5032	0.5224	-0.828	0.5156	0.6351
November	-0.0366	0.3489	0.3724	-1.969	0.2450	0.2511
December	0.1123	0.2102	0.2173	-0.0591	0.1235	0.0869

Table 2: Monthly Blaney-Criddle parameters fitted for GB to reproduce 40-km MORECS (left) and offline MOSES (right) spatial pattern of long-term mean monthly PE (186 grid cells were used). The R^2 statistic gives a measure of the goodness of fit

III. 7. 5. Thornthwaite equation

Thornthwaite correlated mean monthly air temperature with PE as determined by water balance studies in valleys of east-central USA. The original equation is given by Thornthwaite (1948):

$$PE'[mm\ month^{-1}] = 16\left(\frac{10T}{I}\right)^a$$

with T mean monthly temperature [ºC],

$$a = 0.49239 + 0.01792\, I\ - 7.71\ 10^{-5} I^2 + 6.75\ 10^{-7} I^3$$

and $I = \sum_m^{12} \left(\frac{T_m}{5}\right)^{1.514}$ annual heat index and T_m mean temperature of month m [ºC]

This formulation gives unadjusted rates of PE; an adjustment, as a function of the month and latitude (Thornthwaite, 1948), is given by Xu and Singh (2001):

$$PE[mm\ month^{-1}] = PE' \frac{N_m}{12} \frac{D_m}{30}$$

with N_m average daylight hour per day for month m [h] and D_m number of days month m.

It should not be used in arid and semi-arid climates (Jensen et al., 1990).

Section IV Estimation of reference potential evapotranspiration in Britain using observed climate data

IV. 1 Methodological framework

MORECS and offline MOSES PE have been widely used amongst the British hydrological community as reference potential evapotranspiration. However, HadRM3 uses different mathematical equations/ parameters than MORECS or offline MOSES and hence does not provide PE estimates that are equivalent to that of MORECS/MOSES.

To minimise the biases introduced by using modelled climate as input of the hydrological models it is important to use 150-year RCM-driven PE series as close as possible to reference PE used in the calibration of the hydrological models (for both river flow and groundwater level estimation). In addition it is important to use a PE estimation method that can be applied to transient HadRM3 outputs (150-year daily climate time series) and to the UKCIP09 scenarios (monthly climate factors of changes). This is because part of the project concerns comparing Future Flows Hydrology (150-year transient series of river flow and groundwater level) and a larger ensemble of projections of changes including the fuller climate change uncertainty. This relies on using UKCP09 climate change factors to scale the observed climate time series used as input of the hydrological models. As UKCP09 does not include change in PE it is necessary to derive such changes from other climate variables using for example the equations presented in Section III. This means that an alternative formulation that best reproduces the spatio-temporal pattern of MORECS or offline MOSES is required, so that the errors in river flow and groundwater levels simulations due to the use of different estimates of PE are minimised.

This section aims to identify those PE formulations that reasonably reproduce spatial and temporal patterns of MORECS PE, and therefore could be possible candidates for use in this project. One important aspect is to evaluate whether simple formulations, requiring only few climate variables, could provide acceptable substitutes for complex equations. One reason is that some climate variables necessary to estimate PE are not routinely available to climate change impact scientists. Another reason is that some climate data simulated by Global or Regional Climate Models might contain biases – reducing the number of variables to calculate PE might be a way to reduce potential biases in PE estimates.

The majority of the PE equations presented in Section III have been implemented using the same climate input data as used in MORECS, to provide the best like-to-like comparison. Two main characteristics were considered: how well the spatial pattern of PE distribution is reproduced across Britain; and how well the inter-annual variability in PE is reproduced. The results are presented in Section IV. 3.

IV. 2 Data

The MORECS monthly data for each 40 km MORECS square covering Britain are stored on ORACLE Tables within CEH. The variables available for PE estimation are total monthly sunshine hours (hours), mean monthly temperature (degrees C), daytime mean vapour pressure (mb) and daily mean wind speed (miles/day). They will need to be converted in the units of the PE equations.

IV. 3 Reproduction of the spatial distribution of PE across Britain

For each equation, mean monthly PE was estimated using long-term mean monthly climate variables (1961-1990) as input data and compared with MORECS and offline MOSES for the four months typical of winter [January], spring [April], summer [July] and autumn [October].

The maps are presented by month, in decreasing order of complexity/data requirement and investigation done by visual assessment of the maps. Generally the combined methods show the closest correspondence with MORECS for spatial distribution across GB for the four months. The temperature methods, apart from Blaney-Criddle_MORECS, tend to give higher PE, particularly for April and July. Note that offline MOSES has lower PE than MORECS, particularly in January, April and October.

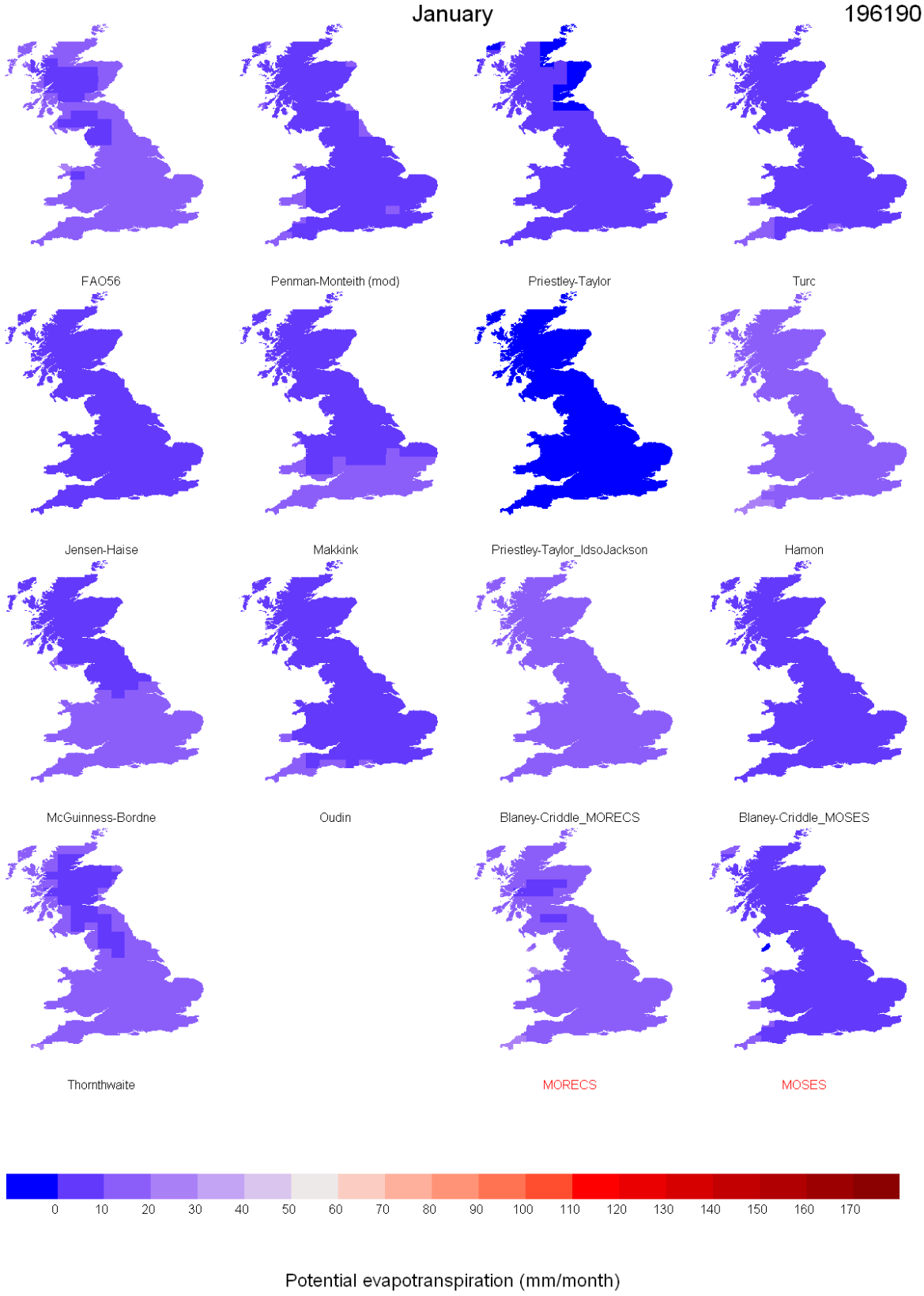

Figure 1: 1961-1990 January. Mean potential evapotranspiration calculated using MORECS climate input. MORECS and offline MOSES mean monthly PE are given as reference

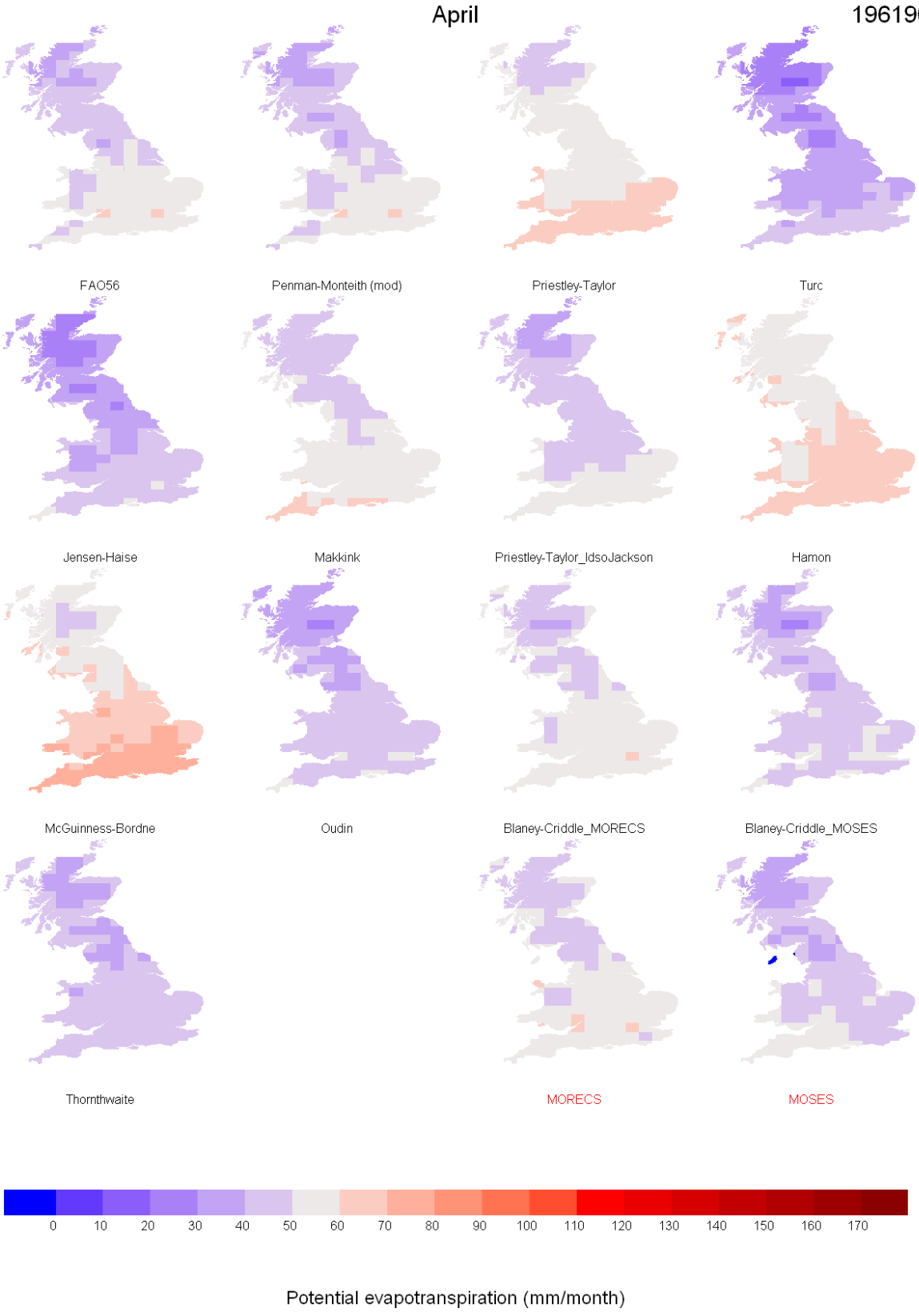

Figure 2: 1961-1990 April. Mean potential evapotranspiration calculated using MORECS climate input. MORECS and offline MOSES mean monthly PE are given as reference

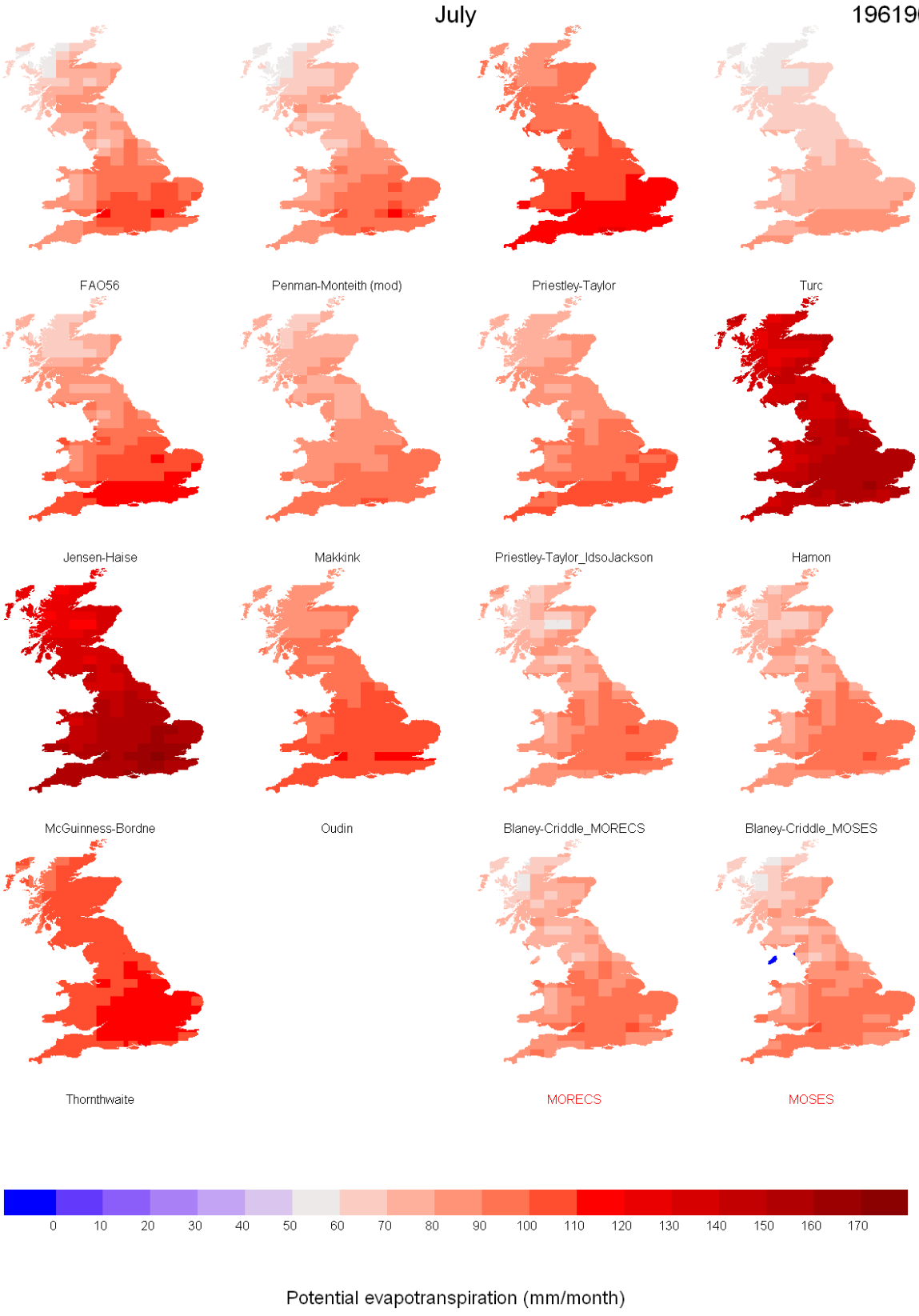

Figure 3: 1961-1990 July. Mean potential evapotranspiration calculated using MORECS climate input. MORECS and offline MOSES mean monthly PE are given as reference

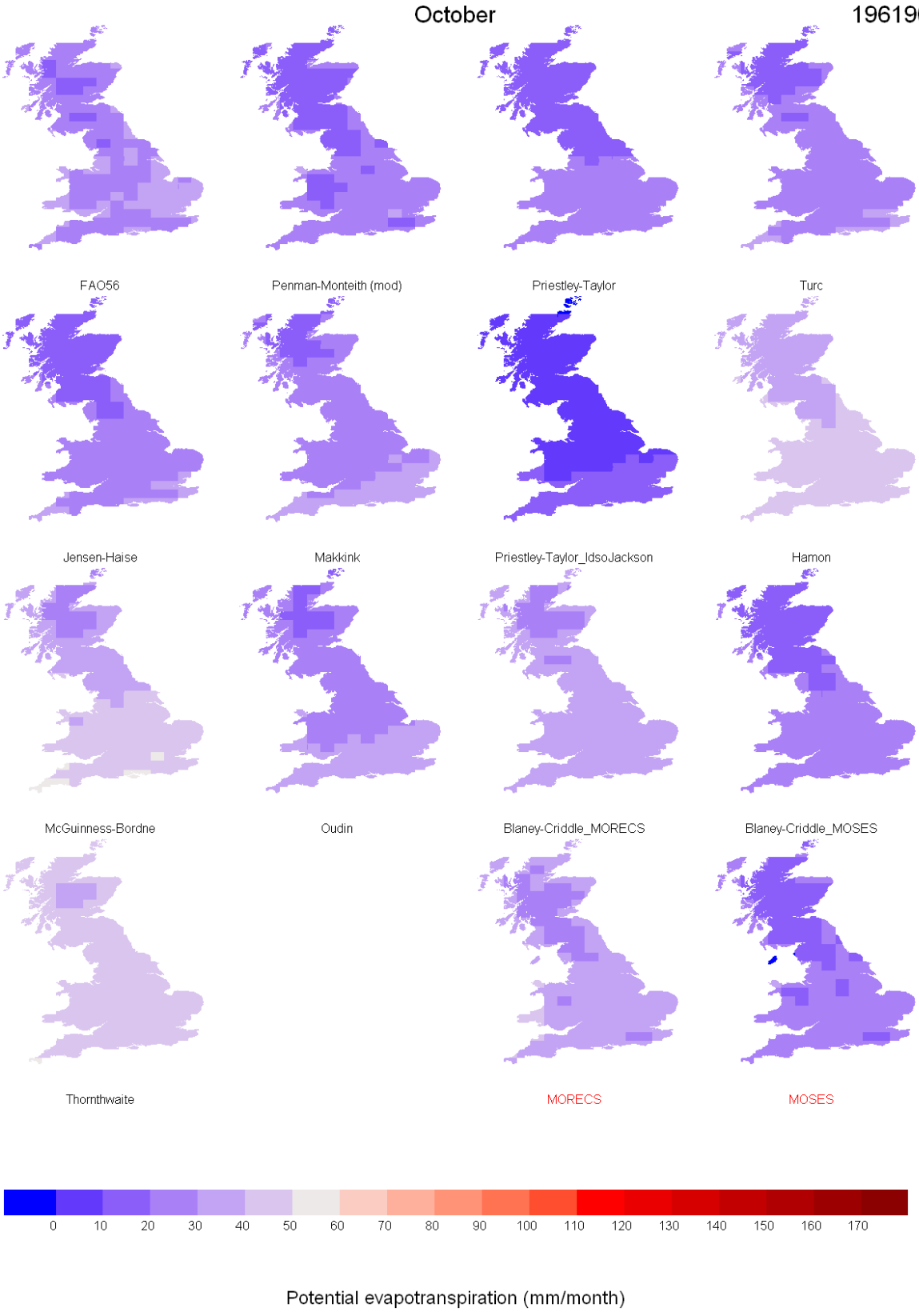

Figure 4: 1961-1990 October. Mean potential evapotranspiration calculated using MORECS climate input. MORECS and offline MOSES mean monthly PE are given as reference

IV. 4 Reproduction of the inter-annual variability of PE across Britain

For each equation, mean monthly PE was estimated using monthly climate variables for two contrasting years as input data and compared with MORECS and offline MOSES for the four months typical of winter [January], spring [April], summer [July] and autumn [October]: 1976, a very dry and hot spring and summer; and 1985, a relatively wet and cool year.

For each contrasting year, the maps are presented by month, in decreasing order of complexity/data requirement. General features of comparability of spatial distribution between the methods are similar to those for the long-term averages for 1961-1990. However, it is only the combined methods (FAO-56 and Penman-Monteith (mod)) which are really able to reproduce the spatial distributions, shown by MORECS for the months of April and July, for the two contrasting years. The radiation methods generally agree more with MORECS than the temperature methods (with the exception of Blaney-Criddle_MORECS). Again, offline MOSES shows generally lower rates of monthly PE than MORECS (and FAO-56).

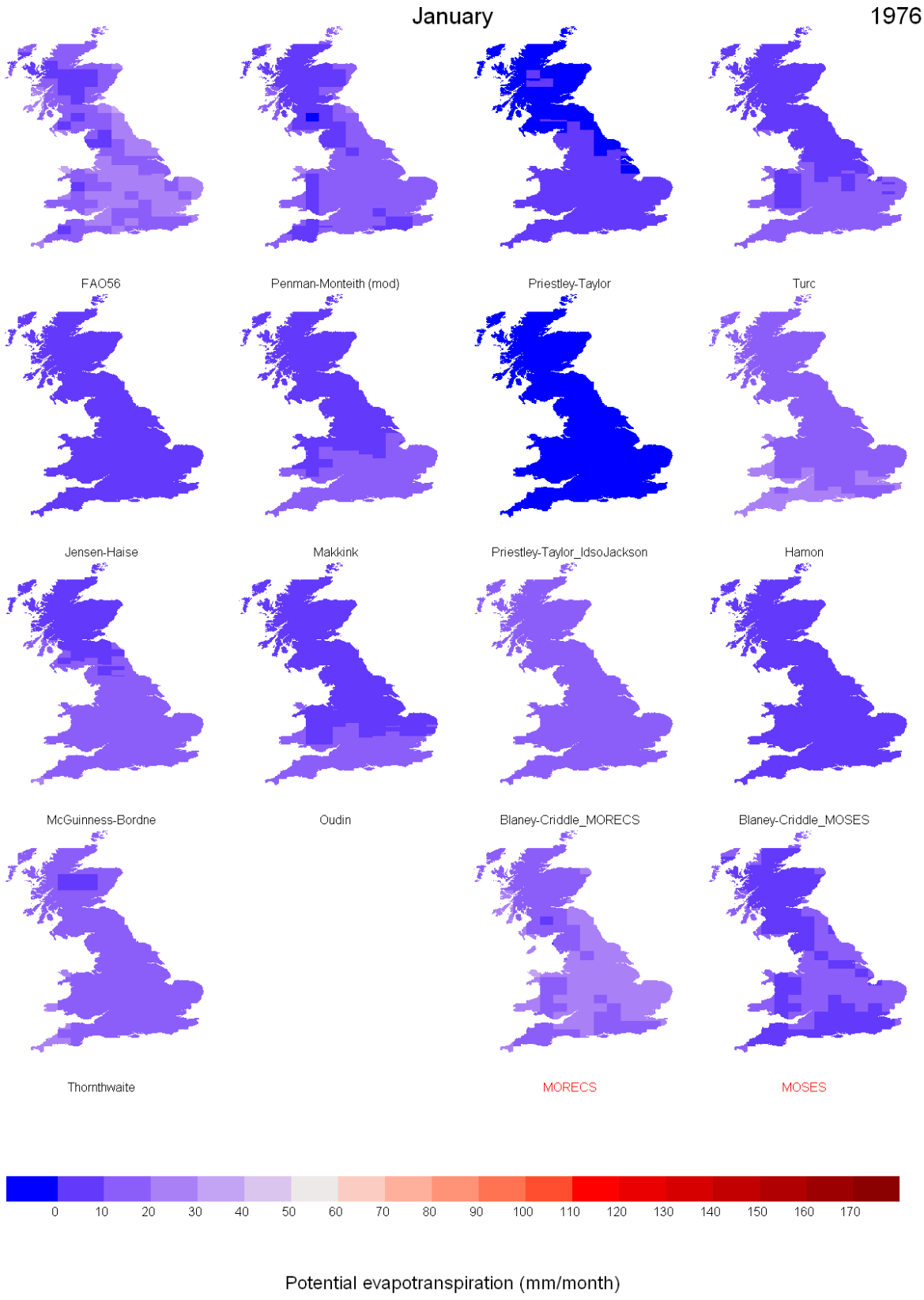

Figure 5: January 1976. Mean potential evapotranspiration calculated using MORECS climate input. MORECS and offline MOSES mean monthly PE are given as reference

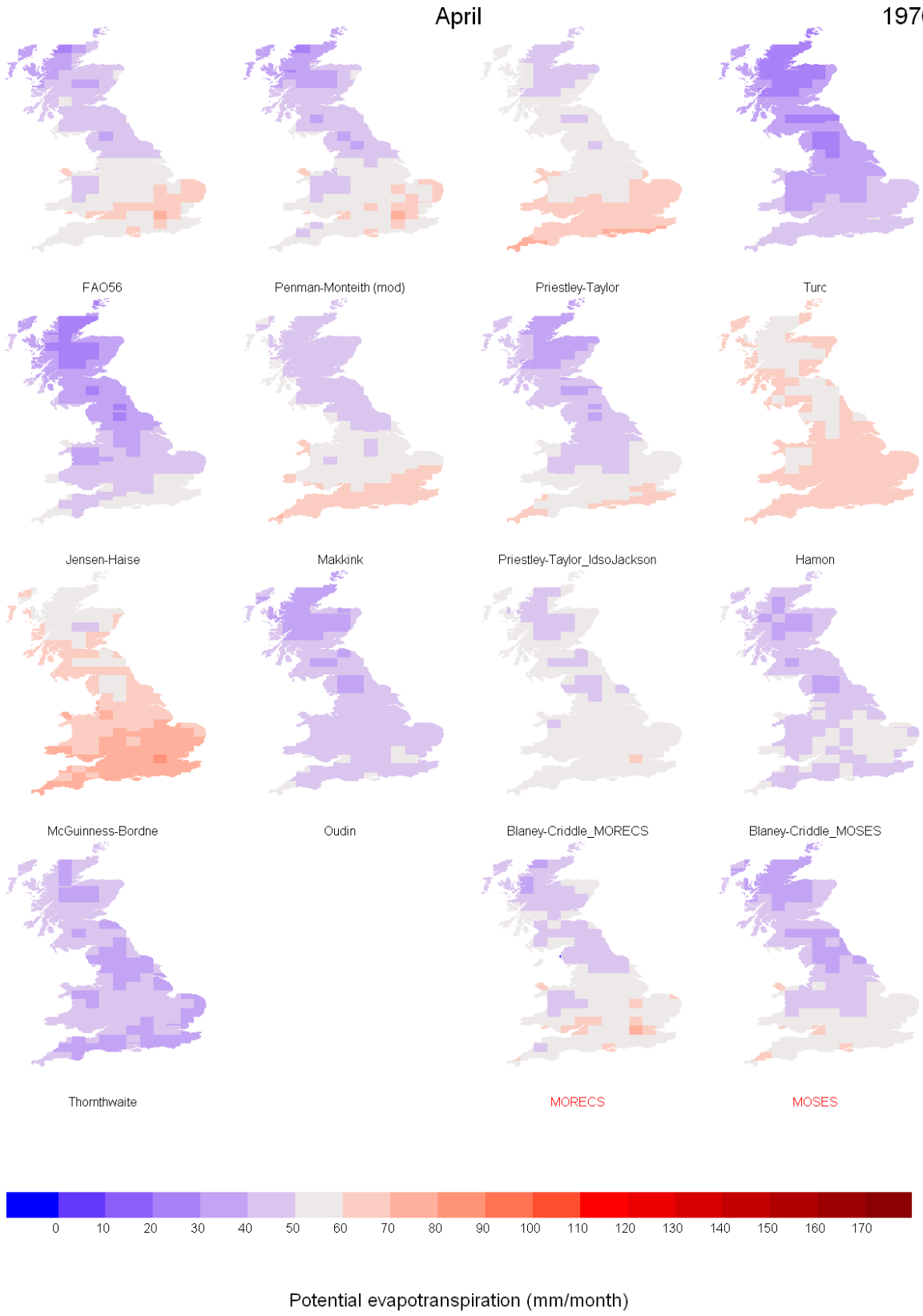

Figure 6: April 1976. Mean potential evapotranspiration calculated using MORECS climate input. MORECS and offline MOSES mean monthly PE are given as reference

Figure 7: July 1976. Mean potential evapotranspiration calculated using MORECS climate input. MORECS and offline MOSES mean monthly PE are given as reference

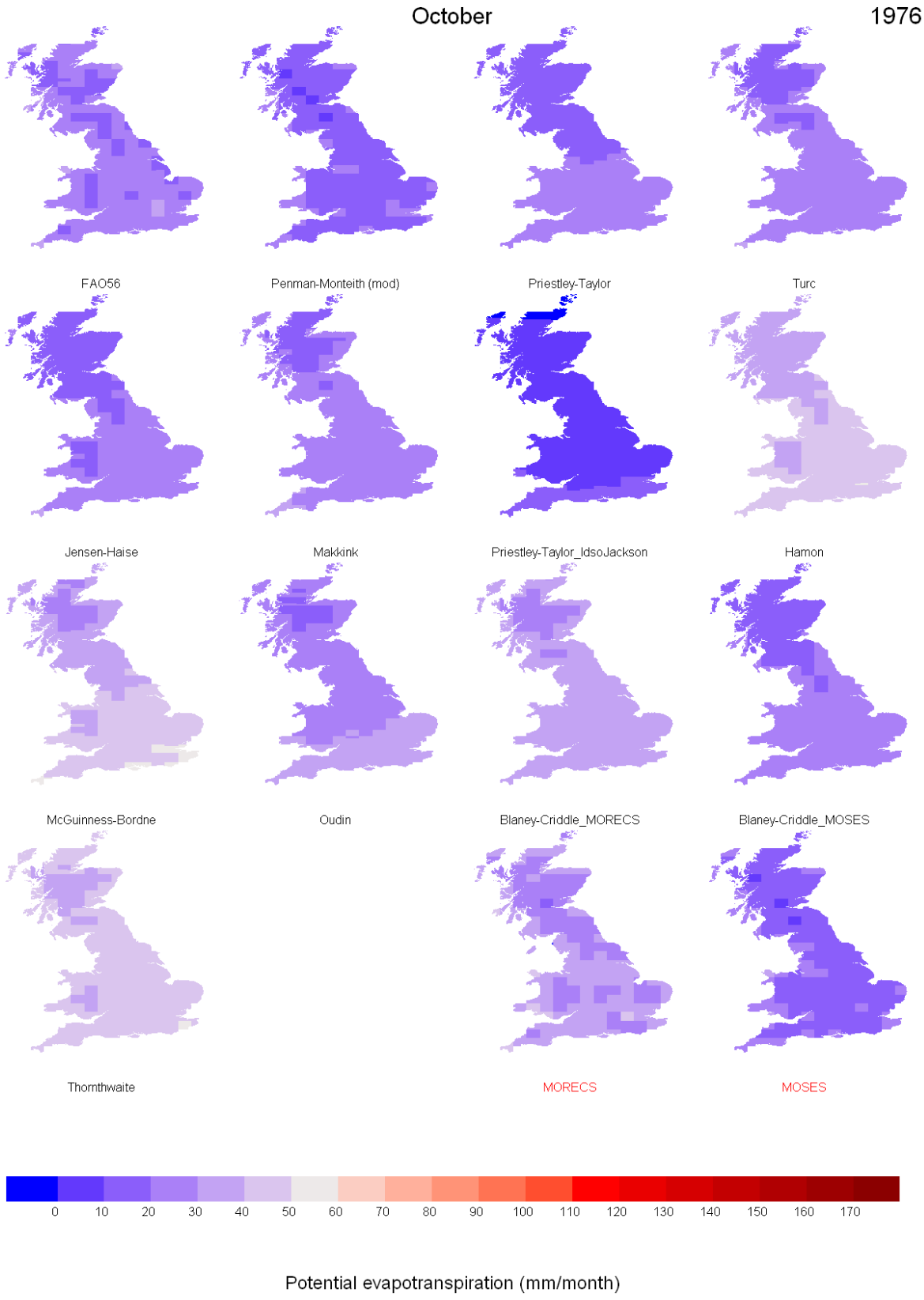

Figure 8: October 1976. Mean potential evapotranspiration calculated using MORECS climate input. MORECS and offline MOSES mean monthly PE are given as reference

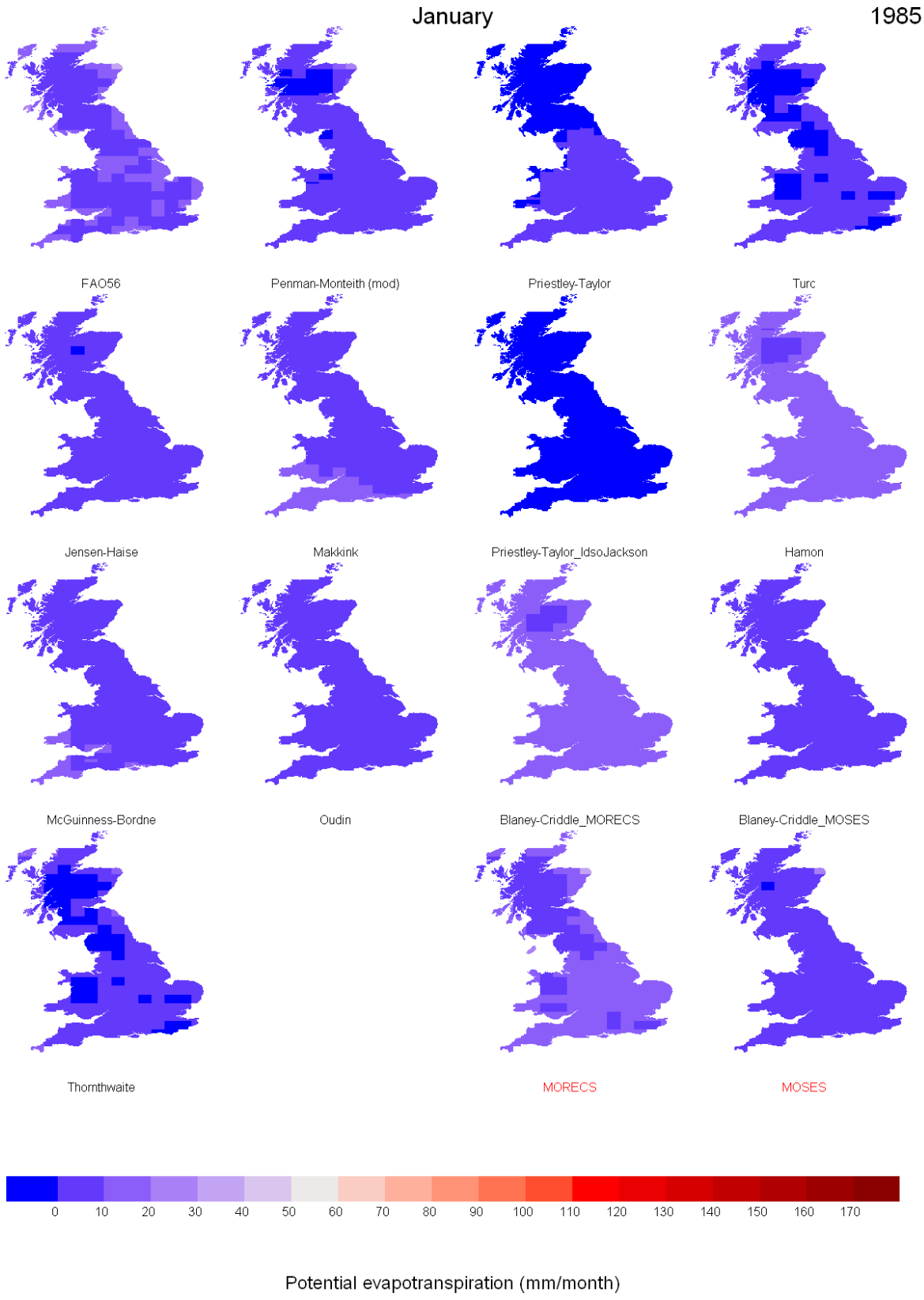

Figure 9: January 1985. Mean potential evapotranspiration calculated using MORECS climate input. MORECS and offline MOSES mean monthly PE are given as reference

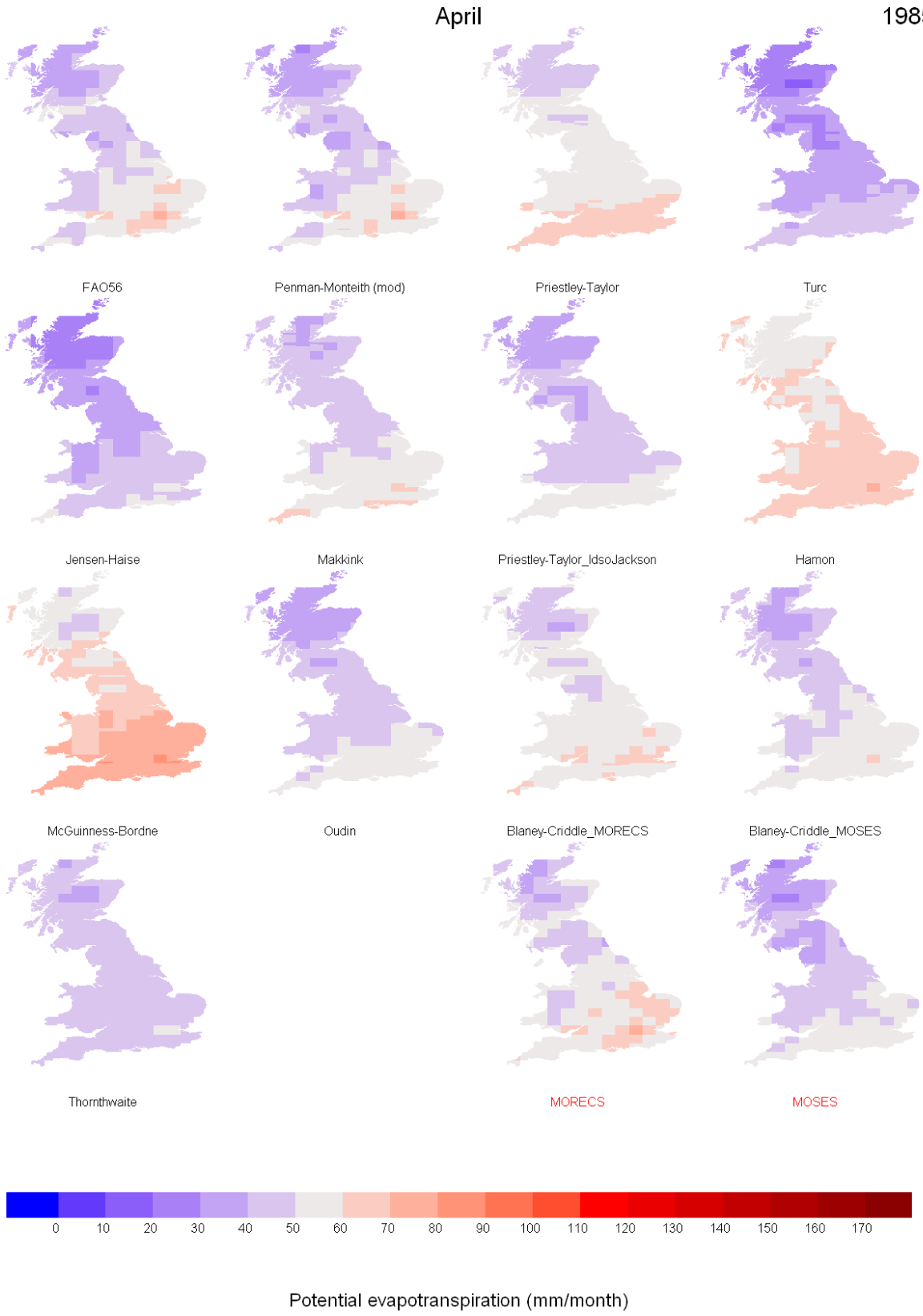

Figure 10: April 1985. Mean potential evapotranspiration calculated using MORECS climate input. MORECS and offline MOSES mean monthly PE are given as reference

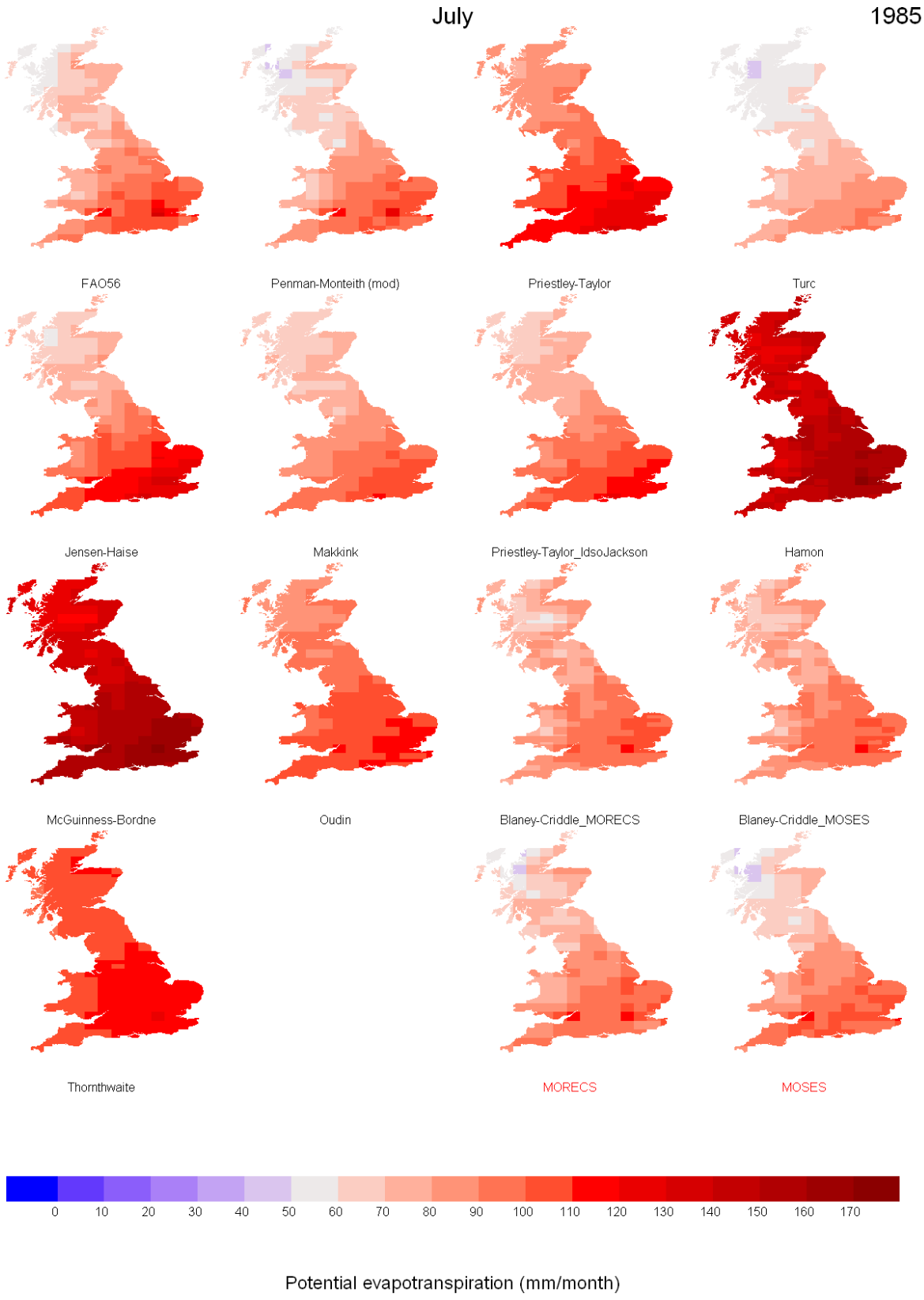

Figure 11: July 1985. Mean potential evapotranspiration calculated using MORECS climate input. MORECS and offline MOSES mean monthly PE are given as reference

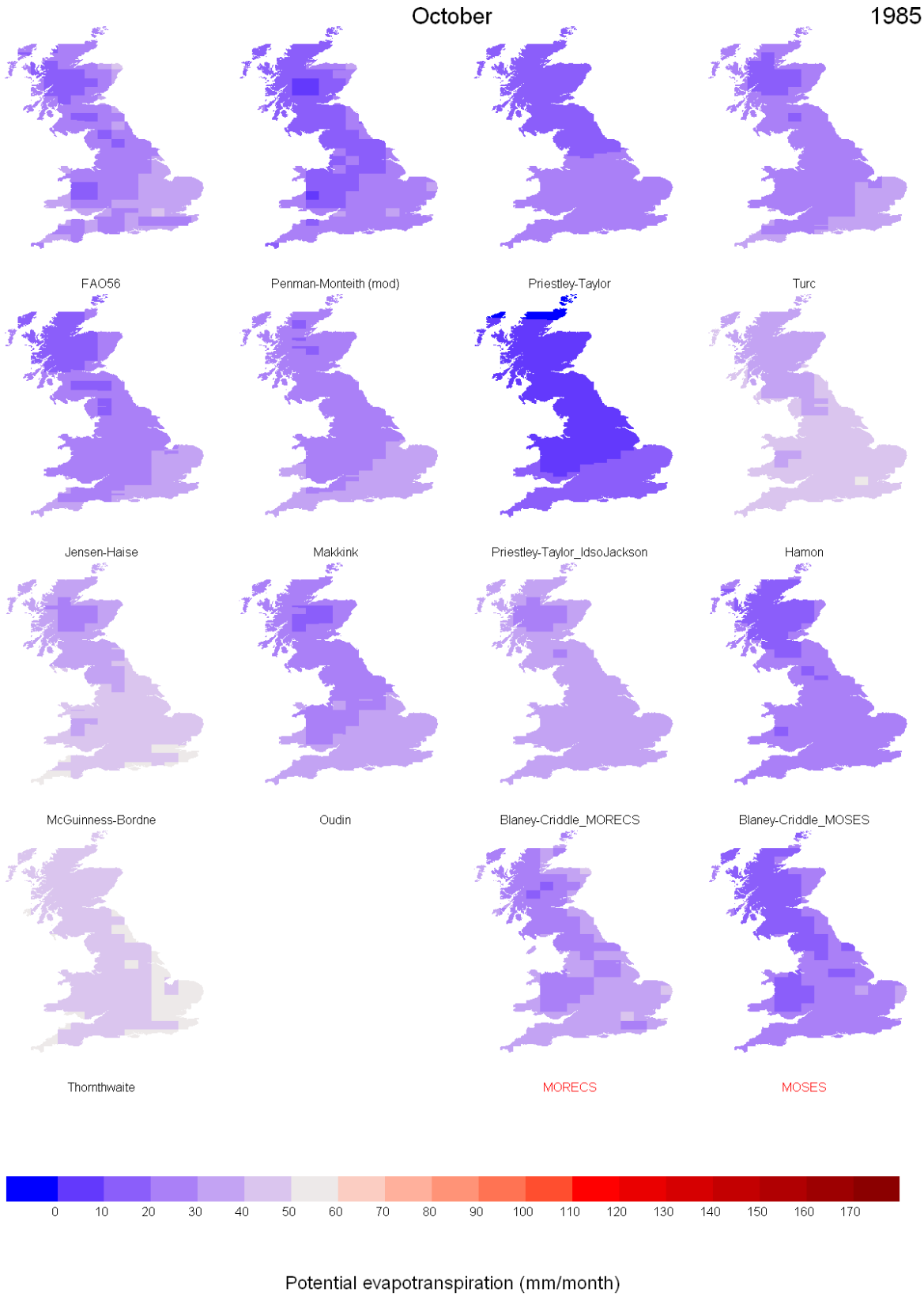

Figure 12: October 1985. Mean potential evapotranspiration calculated using MORECS climate input. MORECS and offline MOSES mean monthly PE are given as reference

Section V Implication for river flow modelling

V. 1 Methodological framework

While the reproduction of the spatio-temporal pattern of MORECS PE is directly relevant for this project, it is the minimisation of errors in river flow estimates that is of critical relevance. In other words, the PE formulation should be chosen so that, for a range of catchments representative of the variety of climatic conditions and catchment characteristics, errors in the simulation of river flows remain acceptable when using both observed and RCM-driven variables. The maps in Figure 1 to Figure 12 show that the complexity of the combined methods is required to fully reproduce the spatial distribution of MORECS PE both for long-term averages and monthly extremes. If the detail of the variation in spatial distribution of PE is not realised, what impact does this have on simulated river flows?

Eight catchments were selected on which to test the hydrological impact of using different formulations of PE. The catchments represent different geographical regions, climatic conditions and catchment properties and are detailed in Table 3. Catchment averages of monthly time series of PE calculated using the formulations given in Sections III. 5, III. 6 and III. 7 and climate data described in Section IV. 2 were used as input to the eight catchments modelled with the PDM (Moore, 2007) and calibrated with MORECS PE. The generated river flow time series are compared with simulations obtained when using MORECS and with observed flow data.

NRFA catchment number	Region	River & location	Flow data start year	Area (km^2)	$SAAR_{6190}$ (mm)	BFI
08004	NE Scotland	Avon @ Delnshaugh	1961	543	1111	0.56
27043	NE England	Wharfe @ Addingham	1973	427	1383	0.33
37001	E England	Roding @ Redbridge	1961	303	606	0.39
40011	SE England	Great Stour @ Horton	1965	345	747	0.70
43005	S England	Avon @ Amesbury	1965	324	745	0.91
50002	SW England	Torridge @ Torrington	1962	663	1186	0.39
64001	Mid Wales	Dyfi @ Dyfi Bridge	1976	471	1834	0.38
94001	NW Scotland	Ewe @ Poolewe	1971	441	2273	0.65

Table 3: Details of the catchments used to test the hydrological impact of the different PE methods

The impact of evaporation on the relationship between rainfall and runoff is likely to be evident through the water balance, determined at a monthly, seasonal or annual time period. It is important in assessing the effect of using different formulations of PE in simulating river flow that appropriate measures are used to quantify the difference. A study by Oudin et al. (2005) to identify the most relevant method to estimate PE for use with rainfall-runoff models concluded that methods based only on temperature were advantageous compared with Penman approaches. Model performance was assessed from a time series measure of fit, the Nash Sutcliffe efficiency, and an overall water balance. However, Nash Sutcliffe efficiency is sensitive to timing and differences between observed and modelled high flows

and overall bias in the water balance may not reveal impacts on seasonal water balance. It is also important to consider that flows are to be simulated using climate change scenarios and therefore the method of calculating PE should preferably not be biased to changes in only some of the contributing factors. Changes in flow indices may differ depending on which PE method is used (Kay and Davies, 2008). The main measure of model performance using the different PE formulations applied here is the impact on mean monthly flow, as an absolute value and as a percentage.

The calibrated model for each catchment was run with daily catchment average rainfall (from observed data) and 14 PE methods for the start year of the flow data given in Table 3 to 1990. The 14 PE methods used to test the impact of method on flow simulation are listed in Table 4. For Priestley Taylor, net radiation was calculated from vapour pressure using equations from Shuttleworth (1993) (named Priestly Taylor (vap) in legends).

Type of PE method	PE name
Combined (Penman based)	FAO-56, Penman-Monteith (mod), MORECS, offline MOSES
Radiation based	Priestley-Taylor, Turc, Jensen-Haise, Makkink, Priestley-Taylor-Idso Jackson
Temperature based	Hamon, McGuinness-Bordne, Oudin, Blaney-Criddle-MORECS, Thornthwaite

Table 4: The 14 PE methods used in the testing, grouped by PE type

V. 2 Results

Comparison of observed and simulated mean monthly flow using 14 PE methods is shown in Figure 13 to Figure 20 for the eight catchments using the PDM model. There are five plots for each catchment with the upper four showing absolute values of mean monthly flow and the lower one showing the difference between observed and simulated expressed as a percentage. The four upper plots have one plot for all methods together, one for the combined methods, one for the radiation based methods and one for the temperature based methods. Initial observations show there is generally a wider spread in simulated mean monthly flow with the radiation and temperature based methods than when using the combined methods. The temperature based methods tend to underestimate the flow (too high evaporation) while radiation based methods are more likely to overestimate the flow (too low evaporation). There is more difference between methods in drier catchments in South and East of England while for wet catchments the method of calculation of PE makes little difference to simulated flow. The difference in pattern of observed and modelled flows during the spring and early summer for catchment 08004 is a consequence of modelling without the snowmelt module, but illustrates the contribution of snowmelt to the seasonal flow regime in mountainous catchments; results when using the snowmelt module are given in a separate report.

From the combined methods offline MOSES and Penman-Monteith (mod) overestimate the mean monthly flow for the three driest catchments (37001, 40011 and 43005) in the winter and spring (too little evaporation), while MORECS and FAO-56 generally provide a good fit in all months. Of the temperature based methods Hamon and McGuiness-Bordne consistently underestimate the mean monthly flow (too much evaporation), while Oudin and Blaney-Criddle-MORECS provide a reasonable representation of monthly variation.

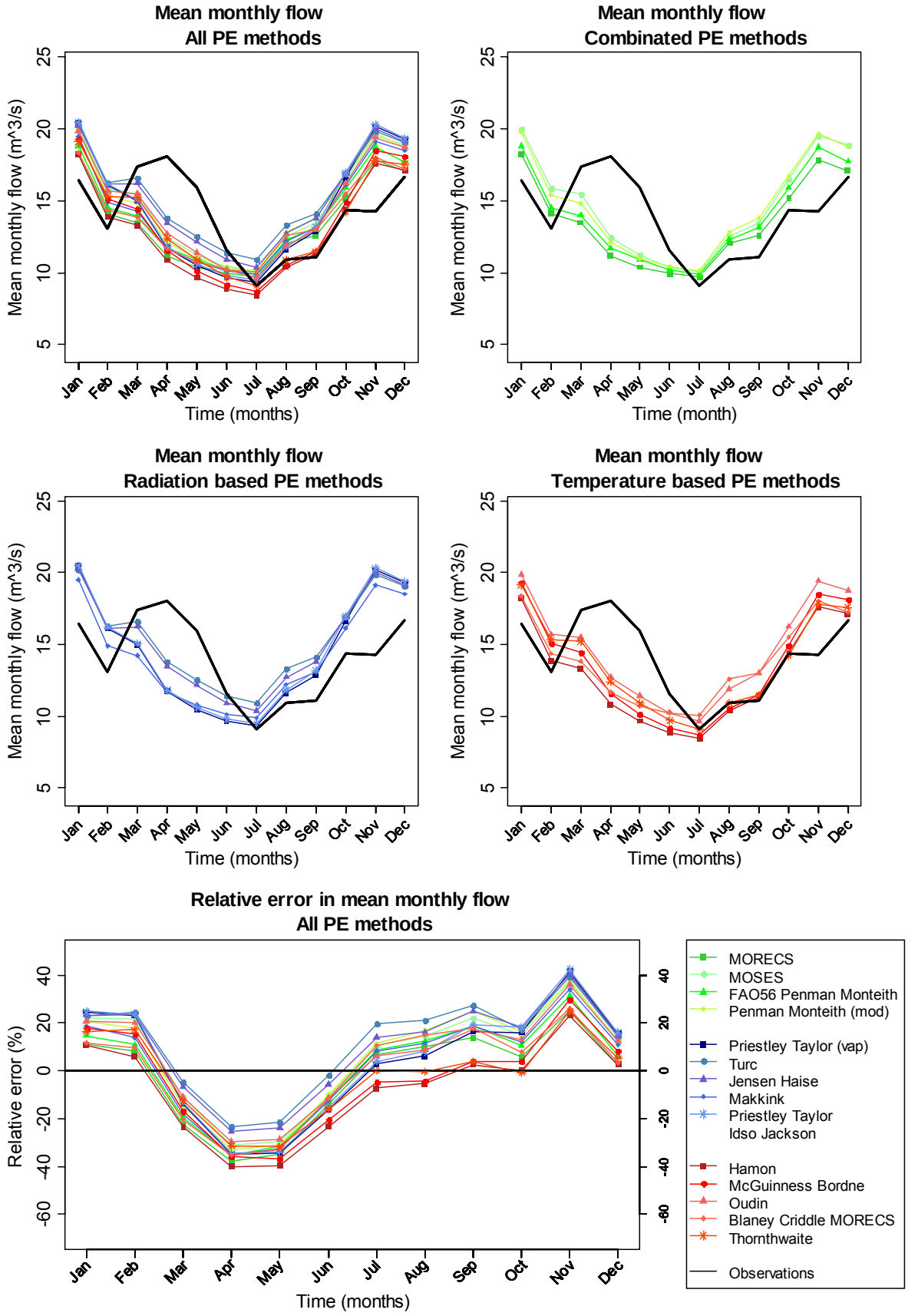

Figure 13: Avon at Delnashaugh (08004). Mean monthly flow calculated using 14 different PE methods compared with mean monthly observed flow (top four graphs); percentage difference between observed and modelled flow (bottom graph).

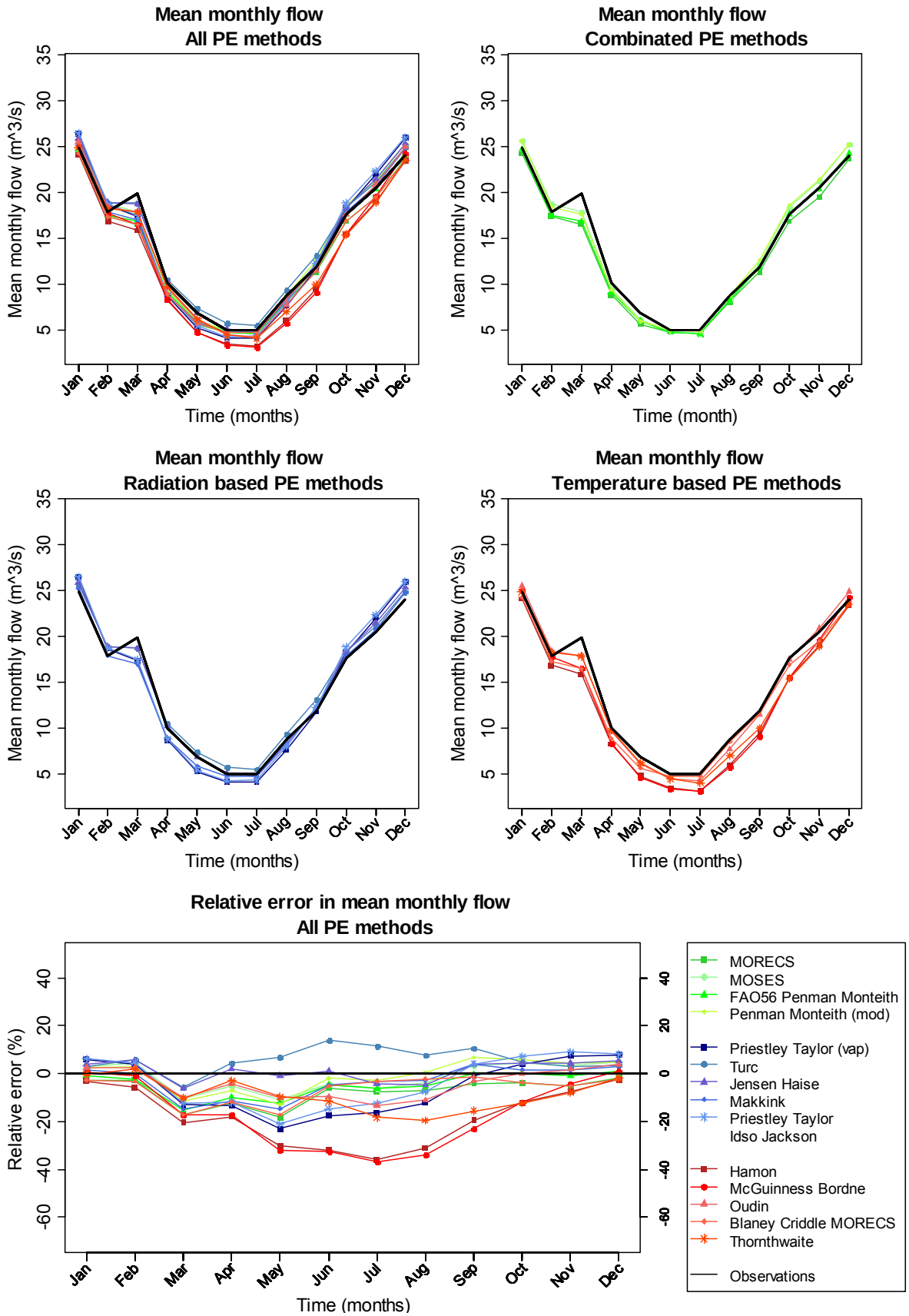

Figure 14: Wharfe at Addingham (27043). Mean monthly flow calculated using 14 different PE methods compared with mean monthly observed flow (top four graphs); percentage difference between observed and modelled flow (bottom graph).

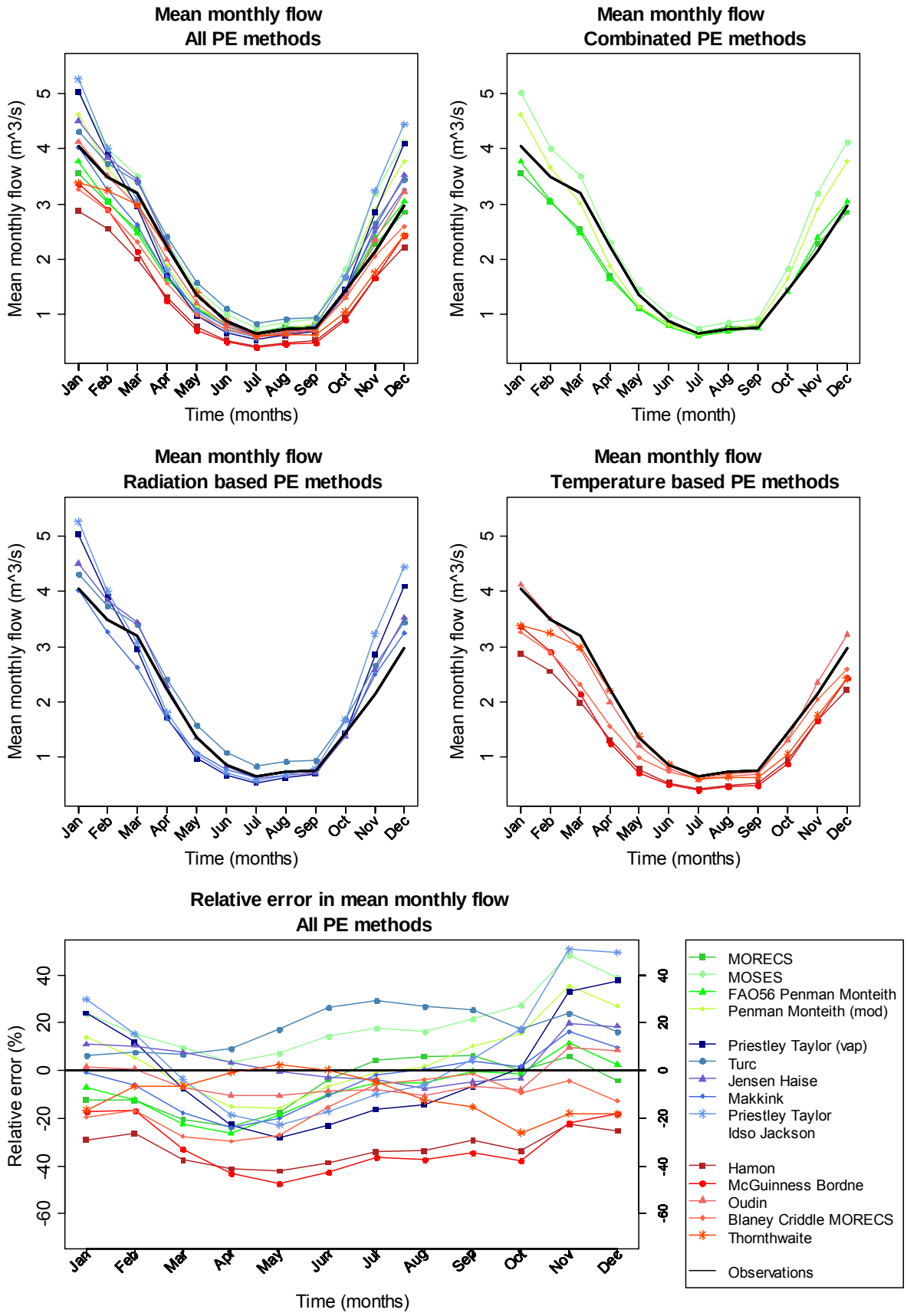

Figure 15: Roding at Redbridge (37001). Mean monthly flow calculated using 14 different PE methods compared with mean monthly observed flow (top four graphs); percentage difference between observed and modelled flow (bottom graph).

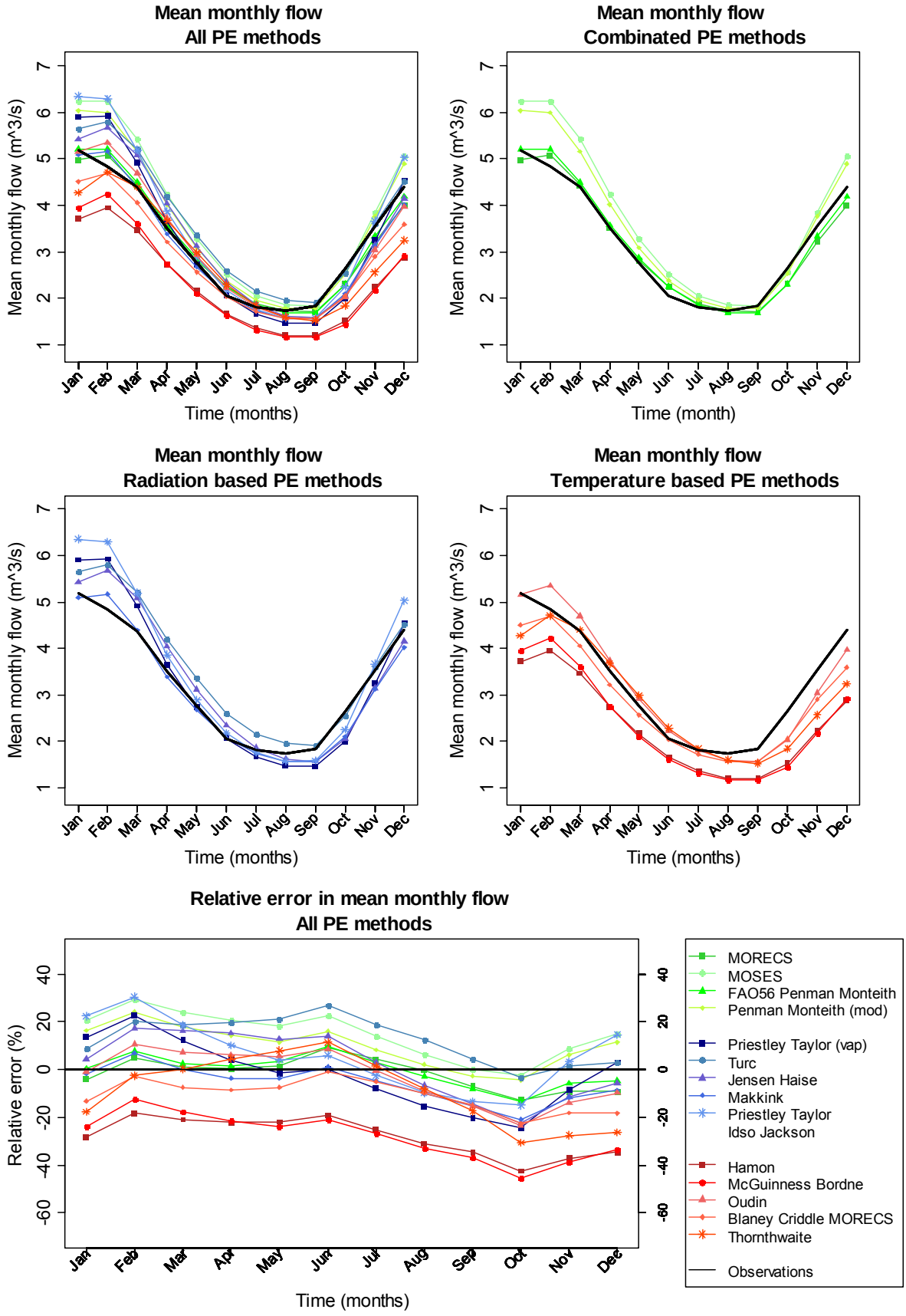

Figure 16: Great Stour at Horton (40011). Mean monthly flow calculated using 14 different PE methods compared with mean monthly observed flow (top four graphs); percentage difference between observed and modelled flow (bottom graph).

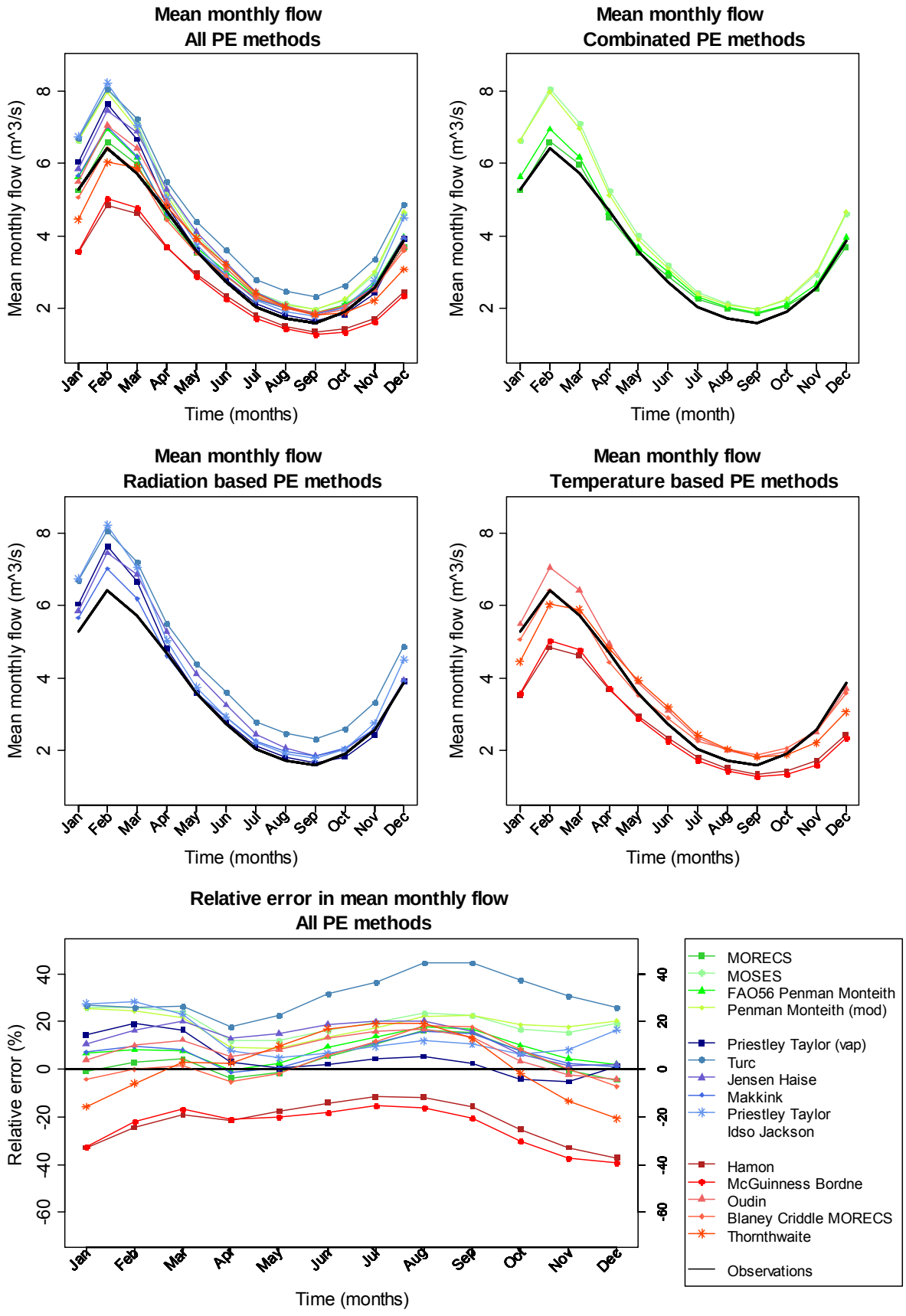

Figure 17: Avon at Amesbury (43005). Mean monthly flow calculated using 14 different PE methods compared with mean monthly observed flow (top four graphs); percentage difference between observed and modelled flow (bottom graph).

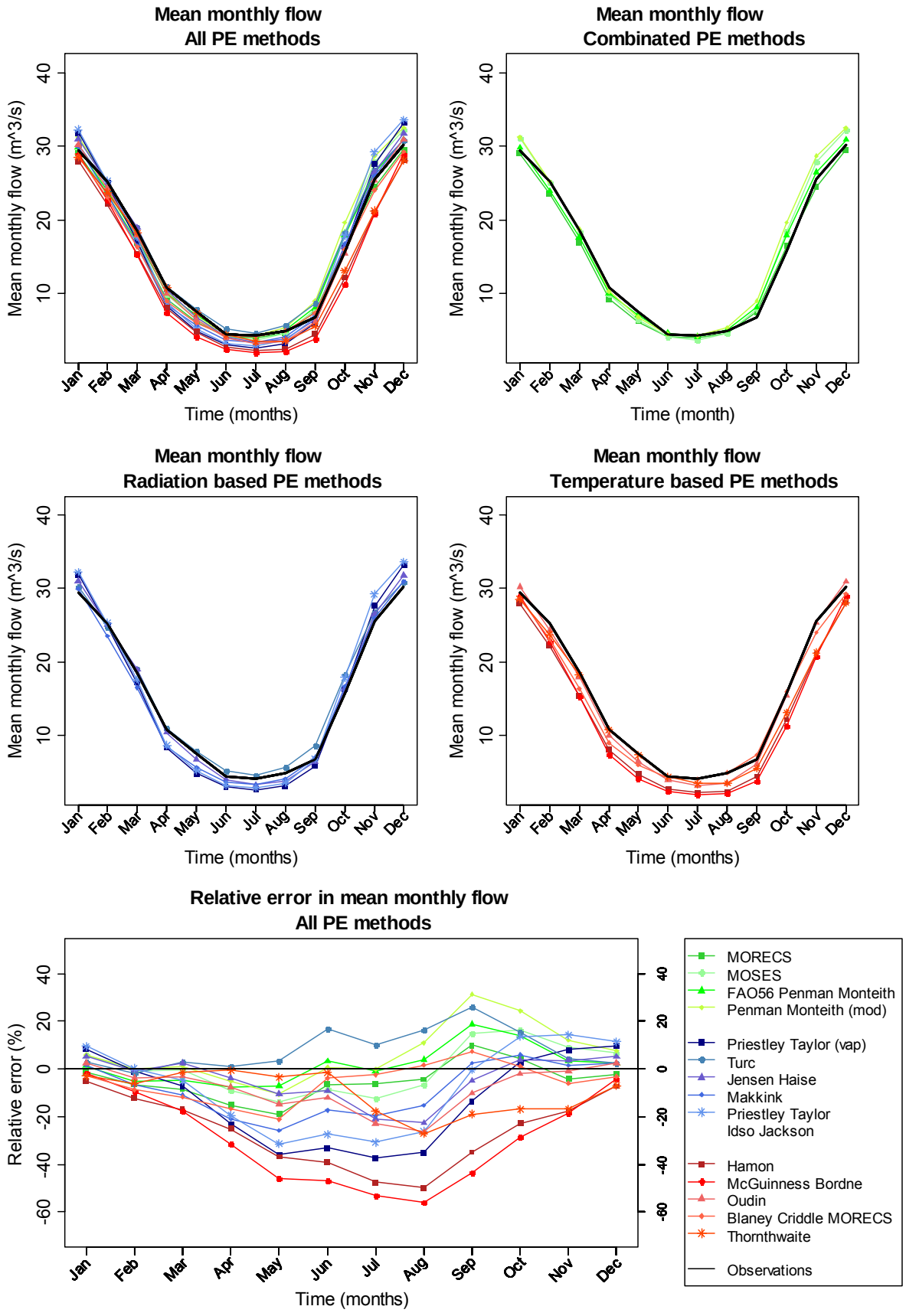

Figure 18: Torridge at Torrington (50002). Mean monthly flow calculated using 14 different PE methods compared with mean monthly observed flow (top four graphs); percentage difference between observed and modelled flow (bottom graph).

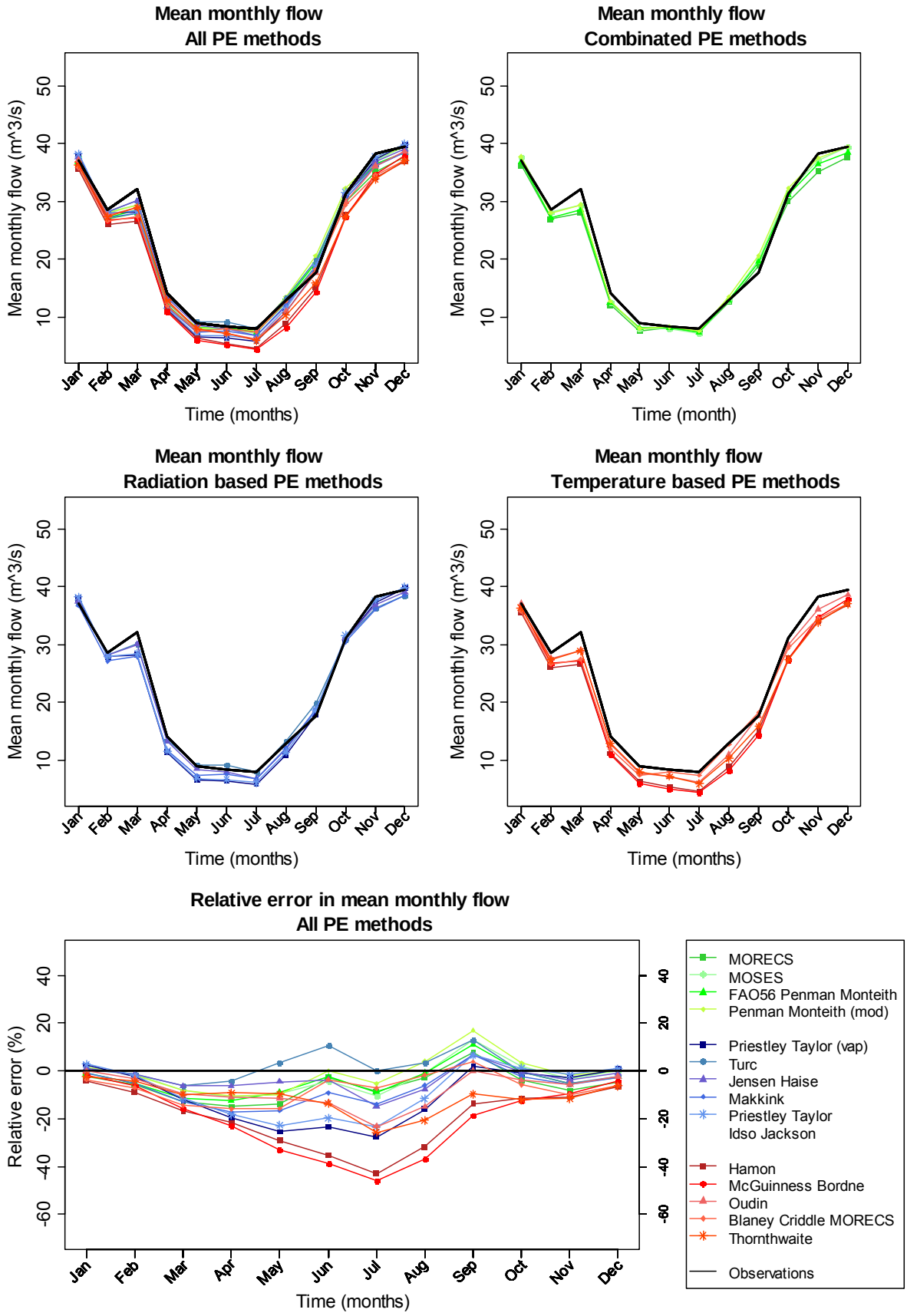

Figure 19: Dyfi at Dyfi Bridge (64001). Mean monthly flow calculated using 14 different PE methods compared with mean monthly observed flow (top four graphs); percentage difference between observed and modelled flow (bottom graph).

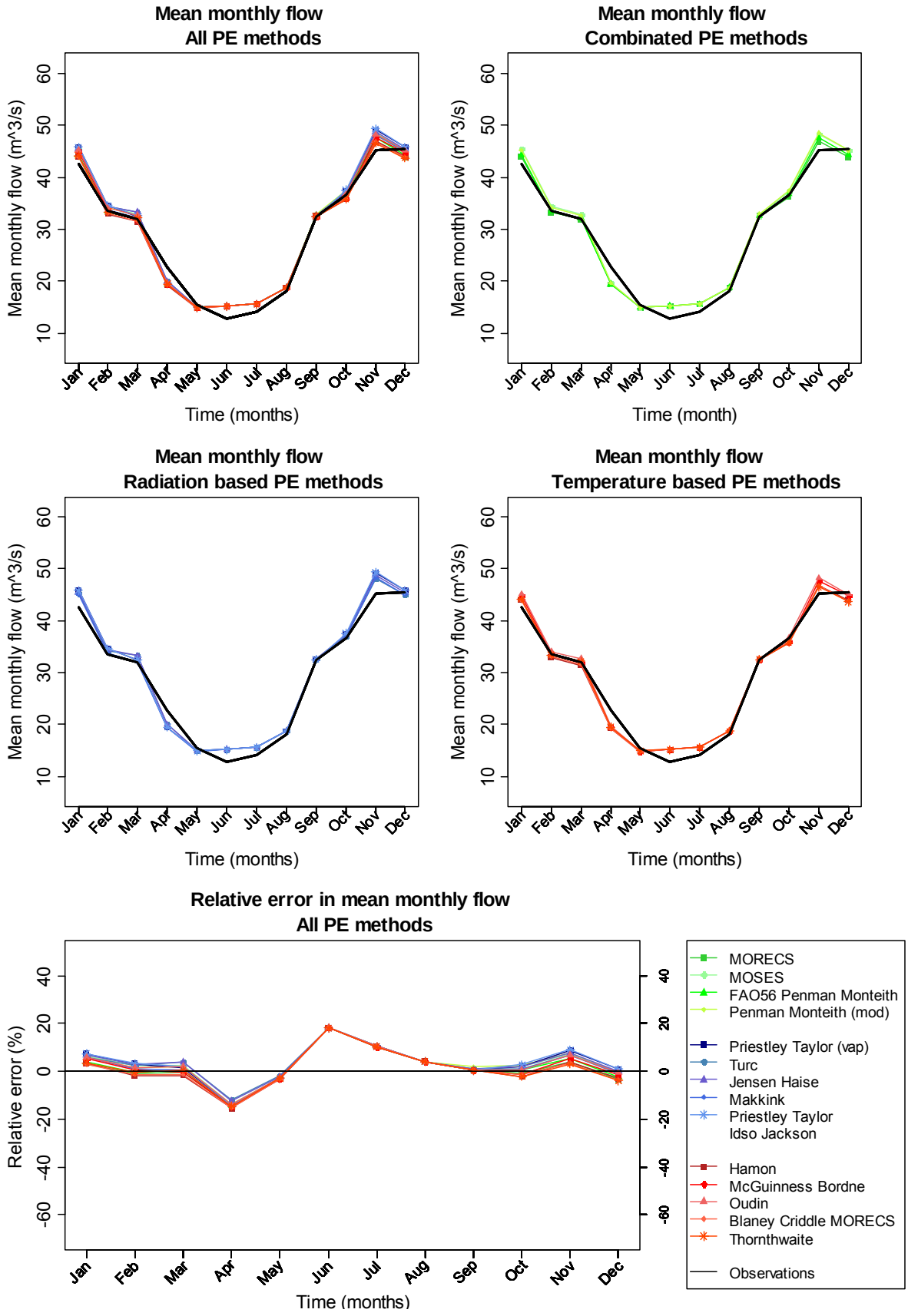

Figure 20: Ewe at Poolewe (94001). Mean monthly flow calculated using 14 different PE methods compared with mean monthly observed flow (top four graphs); percentage difference between observed and modelled flow (bottom graph).

The lower graph in Figure 13 to Figure 20 shows the percentage difference in mean monthly flow between modelled and observed flow for all 14 PE methods. Although absolute differences between observed and simulated mean monthly flows can appear quite small, percentage differences for most catchments lie between ± 40%. For wetter catchments percentage differences are generally lowest in winter and highest in the summer, but may be of similar magnitude throughout the year in drier catchments. A summary of the best performing PE method(s) in each group for each catchment is given in Table 5. Assessment is based on percentage differences and correspondence with MORECS results.

Catchment	Combined methods		Radiation based		Temperature based	
	MORECS	Flow	MORECS	Flow	MORECS	Flow
08004 (Jul–Dec only)	FAO-56	FAO-56	Makkink	Makkink	BC	Thornthwaite
27043	FAO-56	FAO-56	Makkink	Jensen	BC	Oudin
37001	FAO-56	FAO-56	Makkink	Jensen	BC	Oudin
40011	FAO-56	FAO-56	Makkink	Makkink	BC	BC/ Oudin
43005	FAO-56	FAO-56	Makkink	Makkink	BC	BC
50002	FAO-56	FAO-56	Makkink	Makkink/ Jensen	BC	BC
64001	FAO-56	PM_mod	Makkink	Makkink/ Jensen	BC	BC
94001	na	na	na	na	na	na

Table 5: Best PE method from combined, radiation-based and temperature-based groups in comparison with using MORECS PE and with observed flow (BC – Blaney-Criddle-MORECS)

For the combined methods FAO-56 provides the most consistent results. For the radiation and temperature based groups two methods from each stand out as giving the best performance in terms of seasonality of flow – Makkink and Jensen for the radiation methods and Oudin and Blaney-Criddle-MORECS for the temperature methods. The latter is not surprising as the method is calibrated against MORECS data. No preference is given for catchment 94001 as the flow response is dominated by the high rainfall and controlled by outflow from a loch; hence the impact of difference in PE method is very small. Offline MOSES was found to greatly overestimate winter flow (> 30%) in catchments with low SAAR, which shows the impact of the lower PE than with the other combined methods (see the maps for spatial distribution of PE).

To determine the most appropriate method overall from the flow modelling the percentage differences between modelled and observed flow for the six best methods (MORECS, FAO-56, Makkink, Jensen-Haise, Blaney-Criddle-MORECS and Oudin) are shown in Figure 21. The catchments are grouped broadly according to whether they are on the west side of Britain (94001, 64001, 50002, 43005) or east (08004, 27043, 37001, 40011) with north at the top of the page and south at the bottom. The percentage differences are shown together with the mean monthly rainfall and mean monthly PE.

The combination of the graphs in the left and right hand side of Figure 21, for the eight catchments, shows how the seasonal balance between rainfall and PE affects the impact of the different PE calculations on simulated flow. Where the rainfall always exceeds the PE (e.g. catchment 94001) then the impact of the differences in absolute value of calculated PE on flow is limited. Where the average PE in summer is very similar to the rainfall (e.g. 64001, 50002 and 27043) then higher PE results in lower flows – the rainfall is normally sufficient to satisfy a higher evaporative demand. For example, where temperature based methods have higher PE in late summer than other methods the consequent impact with underestimation of flows is evident. Where PE greatly exceeds rainfall, from late spring to early autumn in some catchments (e.g. 37001, 40011 and 43005), then higher PE makes little difference to the simulated flow as rainfall is not sufficient to satisfy the higher demand (AE is similar despite the different PE rates). There is greater difference between the methods for these catchments for January to June than there is for July to December. The examples show how the differences between the PE methods impact on the seasonal hydrological balance and how choice of method may influence how future changes in the seasonal water balance are simulated.

To determine the PE method which performs best overall the average of the 12 monthly percentage differences between observed and simulated mean monthly flow was calculated for each catchment for the six methods used in Figure 21. The average percentages are given in Table 6 where the two columns for each method give the relative and absolute errors. The relative average includes the sign of the difference (i.e. positive or negative) in the calculation whereas the absolute is the average of the absolute errors. The relative errors, therefore, indicate the net bias over a year while the absolute errors provide the average monthly difference through the year. Where the errors are the same for relative and absolute then all the 12 monthly percentage differences have the same bias. The best and worst performing method is indicated for each catchment by blue (good) and red (bad) shading using the absolute average errors as the primary indicator (see Table 6). MORECS values are given for comparison. The mean error from all eight catchment is given in the bottom row. The errors in Table 6 show that all methods apart from FAO-56 perform worst for at least one catchment, with Jensen-Haise being the most variable (best for two catchments and worst for four). Blaney-Criddle-MORECS has similar performance to MORECS for five of the catchments but is less good for two of them. From the overall mean Blaney-Criddle-MORECS does less well than either Makkink or Oudin. The method with the best overall mean is FAO-56 though the relative differences between the methods are quite small.

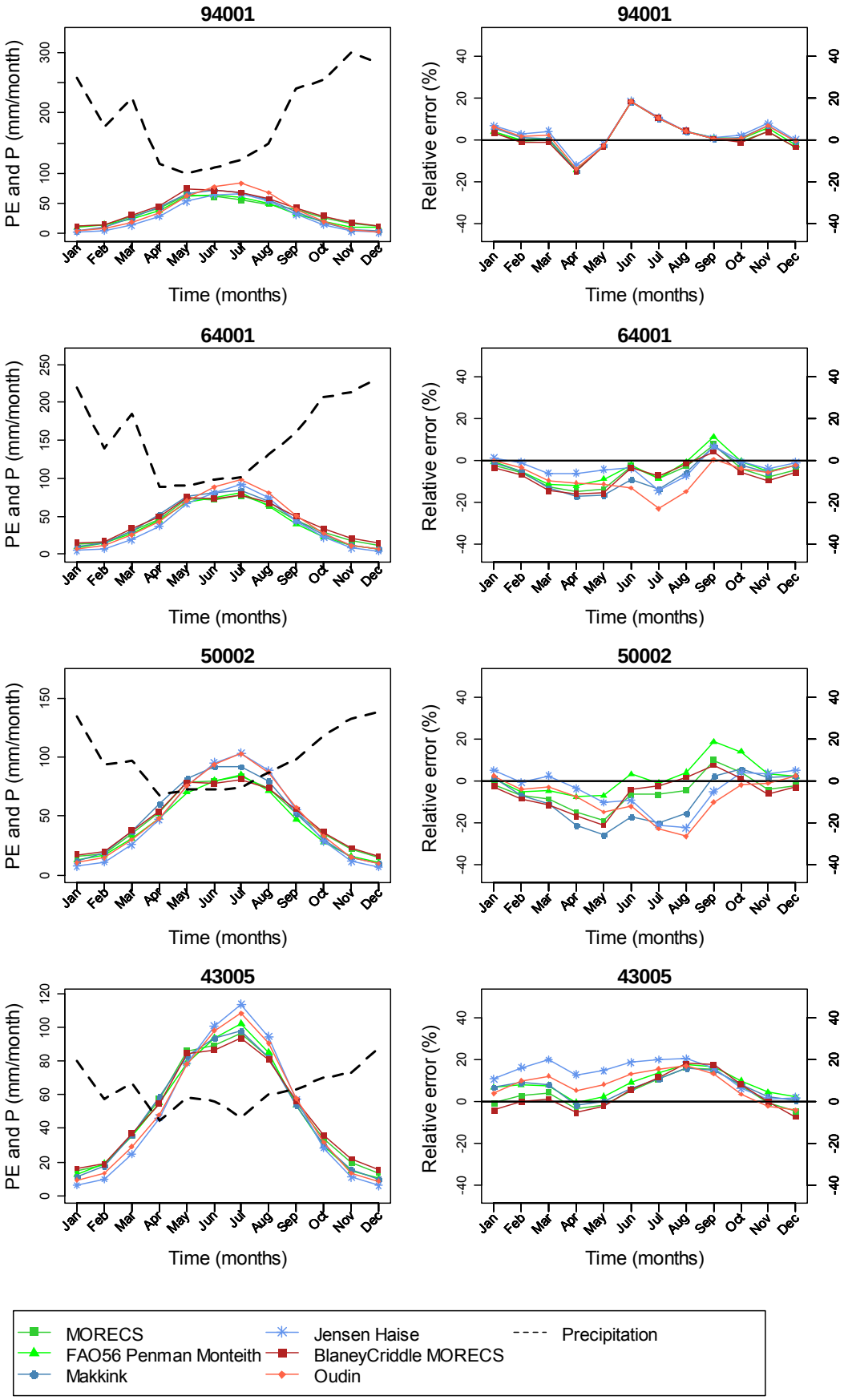

Figure 21: Comparison of mean monthly precipitation and PE (left) and percentage difference between observed and modelled mean monthly flow (right)

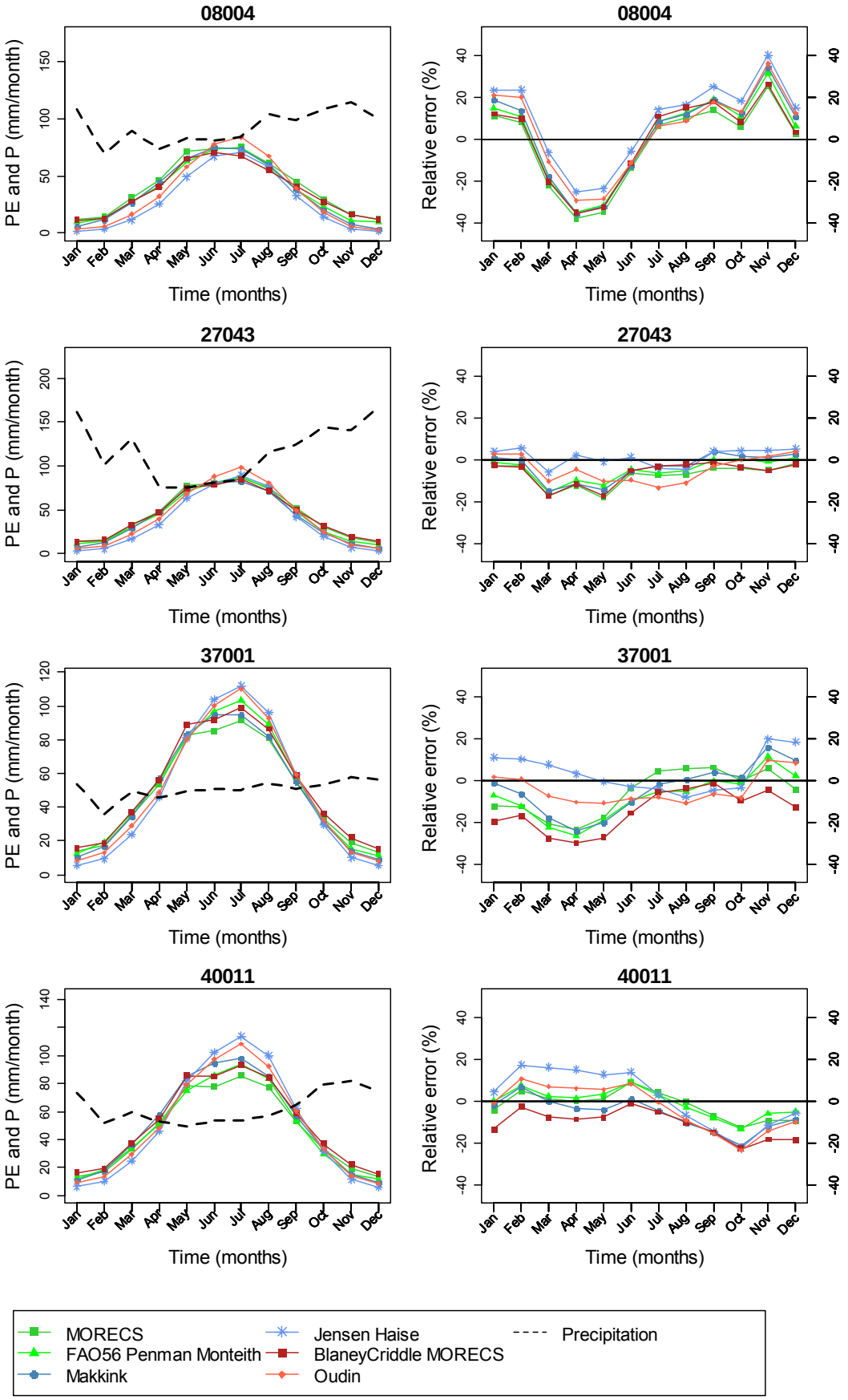

Figure 21 (cont.)

Catchment	Morecs		FAO-56		Makkink		Jensen-Haise		BC-Morecs		Oudin	
	Rel (%)	Abs (%)	Rel (%)	Abs (%)	Rel (%)	Abs (%)	Rel (%)	Abs (%)	Rel (%)	Abs (%)	Rel (%)	Abs (%)
08004(Jul-Dec)	10.5	10.5	14.7	14.7	15.9	15.9	21.3	21.3	13.4	13.4	15.6	15.6
27043	-7.4	7.4	-4.8	5.0	-3.4	5.2	1.2	3.9	-6.3	6.3	-4.3	6.1
37001	-6.0	9.7	-7.9	10.2	-4.2	9.4	3.9	7.8	-14.5	14.5	-4.2	7.6
40011	-1.8	5.3	-0.6	5.2	-6.0	7.4	1.8	12.0	-10.8	10.8	-2.9	9.2
43005	4.2	6.1	8.2	8.3	6.9	7.1	13.2	13.2	3.6	6.8	8.0	9.0
50002	-5.0	7.4	1.7	6.0	-8.6	10.9	-4.4	7.8	-5.6	7.3	-8.3	9.1
64001	-6.1	7.4	-4.0	5.8	-7.2	8.3	-3.5	4.8	-7.3	7.9	-8.3	8.3
94001	1.3	5.3	1.9	5.3	2.4	5.5	3.5	5.9	1.1	5.4	2.7	5.6
Mean	-1.3	7.4	1.2	7.6	-0.5	8.7	4.6	9.6	-3.3	9.1	-0.2	8.8

Table 6: Average percentage difference between observed and modelled mean monthly flow (Jan to Dec). Rel=allowing for sign (+ or -), Abs=no allowance for sign (i.e. absolute value)

Section VI Estimation of reference potential evapotranspiration in Britain using RCM climate data

VI. 1 Methodological framework

The same equations implemented in Section IV were used with input climate data obtained directly from the RCM, to evaluate the impact that possible existing biases in RCM climate might have on the estimation of PE. PE has been calculated for one HadRM3-PPE run, afgcx, using data for 1961 to 1990.

Current generation RCMs are not always able to reproduce accurately some climate variables. This issue is well known for precipitation, and has been mentioned for other variables such as wind speed, for example. While not directly concerned with the accuracy of the RCM climate, it is important that such possible biases in RCM climate do not impact significantly on the estimation of PE. In particular, the use of complex equations, which might be the best way to reproduce the physical mechanisms of PE, and by extension, produce the best approximation of MORECS and offline MOSES PE, might rely on climate variables which are not well simulated by HadRM3-PPE, and thus could, when used with RCM output variables instead of observations, produce poorer approximations of MORECS and offline MOSES PE than a simpler method (e.g. which depends only on climate variables better simulated by RCMs, such as temperature). Because RCM simulations are not designed to reproduce the weather nor the exact historical climate variation, it is not possible to test the PE formulation on specific years. Note that for combined equations RCM wind speed is used as an input variable in this section.

This section aims to evaluate which PE formulations provide reasonably good reproduction of the spatial distribution of long-term mean monthly MORECS and offline MOSES PE using RCM climate input variables. Two main characteristics were considered: how well the spatial pattern of PE distribution is reproduced across Britain; and for radiation-based formulation, how well the spatial pattern of PE distribution is reproduced across Britain when deriving radiation from other climate variables compared to direct RCM radiation. This is because probabilistic changes in radiation (long and short wave) are not calculated in the same batch as precipitation and temperature, and hence, cannot be used to estimate PE for the probabilistic assessment of river flow changes.

VI. 2 Data

The input variables used in this section, and their corresponding name and stash code in HadRM3 outputs, are given in Table 7. Note that for temperature, the RCM output was not used directly, but a bias-corrected version was used. It consists of a 5-km monthly linear correction estimated from the 5-km UKCP09 temperature dataset and was applied to the daily temperature for each HadRM3 grid cell, hence also providing a downscaling of the data. As no UK gridded observed time series other than temperature and precipitation were available to us at the time of the study no bias correction could be done for any other climate variables.

Variable	RCM code name	RCM stash code	Unit	UKCP09 Set
Mean daily temperature	tas	M1s3i236	ºK	1
Relative humidity	hurs_pc	M1s3i245	%	1
Total cloud (cloudiness fraction)	Total_cloud_lw_rad	M1s2i204	Fraction	1
Net surface long wave flux	longwave	M1s2i201	W m^{-2}	2
Net surface short wave flux	solar	M1s1i201	W m^{-2}	2
Wind speed	wss	M1s3i249	M s^{-1}	-

Table 7: HadRCM3-PPE climate variables used to estimate UK PE. Last column indicates the set of the UKCP09 probabilistic samples where change factors are available

Some PE equations require input data not directly available from HadRM3-PPE but which were derived from climate variables listed in Table 7 using the relationships presented in Section III. 4.

VI. 3 Reproduction of the spatial distribution of PE across GB without RCM radiation

For each equation, mean monthly PE was estimated using long-term RCM mean monthly climate variables as input data and compared with MORECS and offline MOSES for the four months typical of winter [January], spring [April], summer [July] and autumn [October]. Radiation (short and long wave) was derived from other climate variables using the Shuttleworth (1993) equations rather than using HadRM3 radiation estimates (see Section III. 4. 22.).

The maps are presented by month, in decreasing order of complexity/data requirement. Generally, BC-MORECS best reproduces MORECS PE patterns all year round but does show an underestimation of July PE in upland areas. FAO-56 also reproduces well the MORECS PE but does tend to underestimate some of the spatial variation in Britain.

In April, BC-MORECS and FAO-56 reproduce best the overall MORECS pattern. MORECS PE is overestimated over the whole of Britain by Penman-Montieth (mod), some radiation methods (both versions of Priestley-Taylor and Makkink) and some temperature methods (Hamon and McGuinness-Bordne), while it is underestimated by Turc, Jensen-Haise, Oudin, BC-offline MOSES and Thorthwaite. In July, all equations overestimate PE except BC-MORECS and BC-offline MOSES; however, both show a strong underestimation of PE in high lands, and a somehow unrealistic gradient from low to high PE. In October, BC-MORECS reproduces best MORECS PE, with combined and radiation methods generally underestimating MORECS PE and temperature methods overestimating MORECS PE except Oudin and BC-offline MOSES. Note that BC-offline MOSES and Turc resemble offline MOSES PE.

When looking at the five PE methods highlighted as the most appropriate to use for river flow estimation in IV. 4 (FAO-56, Makkink, Jensen-Haise, BC-MORECS and Oudin), only BC-MORECS provides arguably the best PE estimates when using RCM data, but does show in July an overestimated PE range. The combined method FAO-56 also provides reasonably good estimates, albeit overestimating PE in July and October.

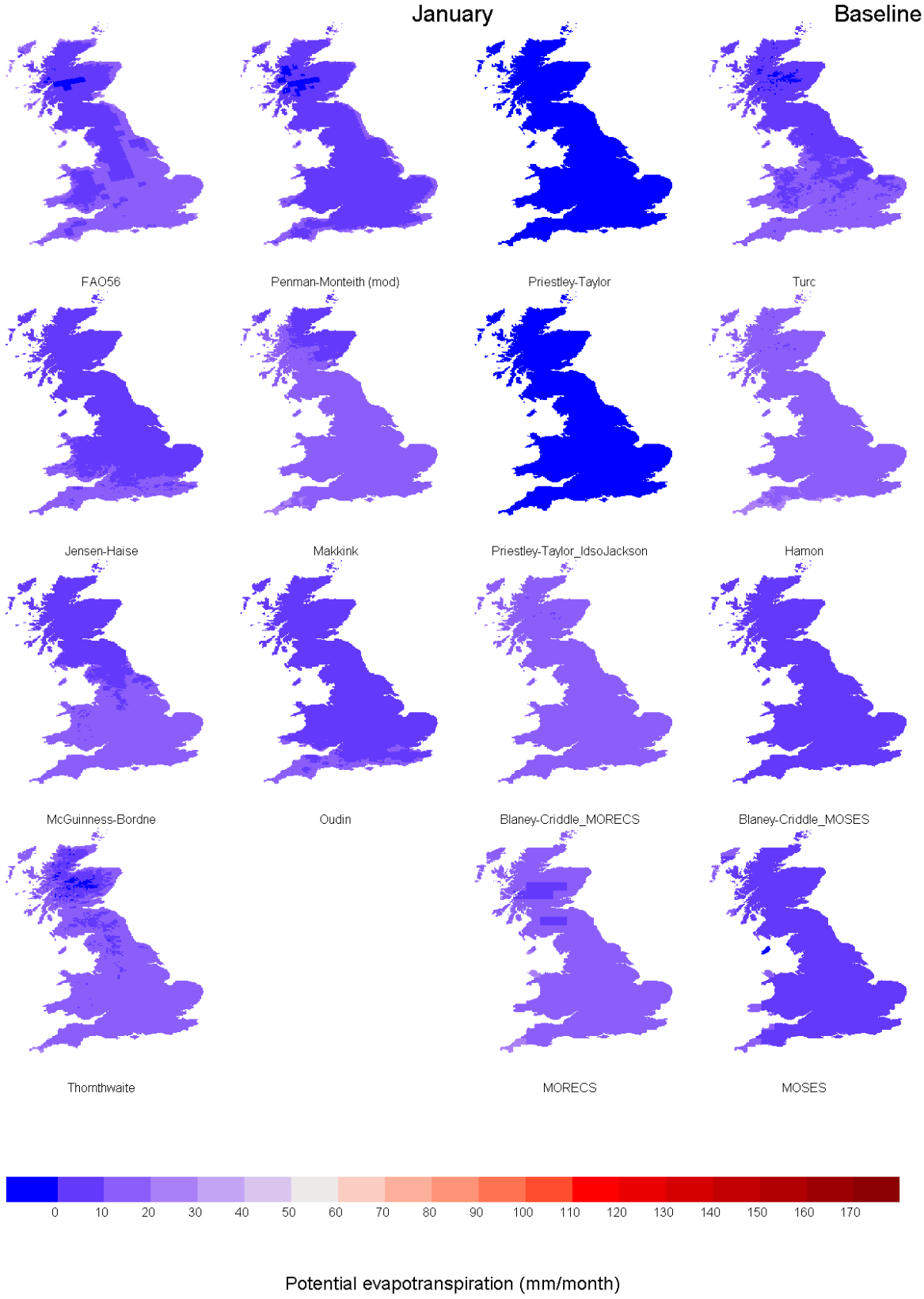

Figure 22: January mean. Potential evapotranspiration derived using HadRM3-afgcx climate data for the baseline period 1961-1990 using 13 PE equations and reference MORECS and offline MOSES PE. Radiation is derived from Shuttleworth (1993) equations

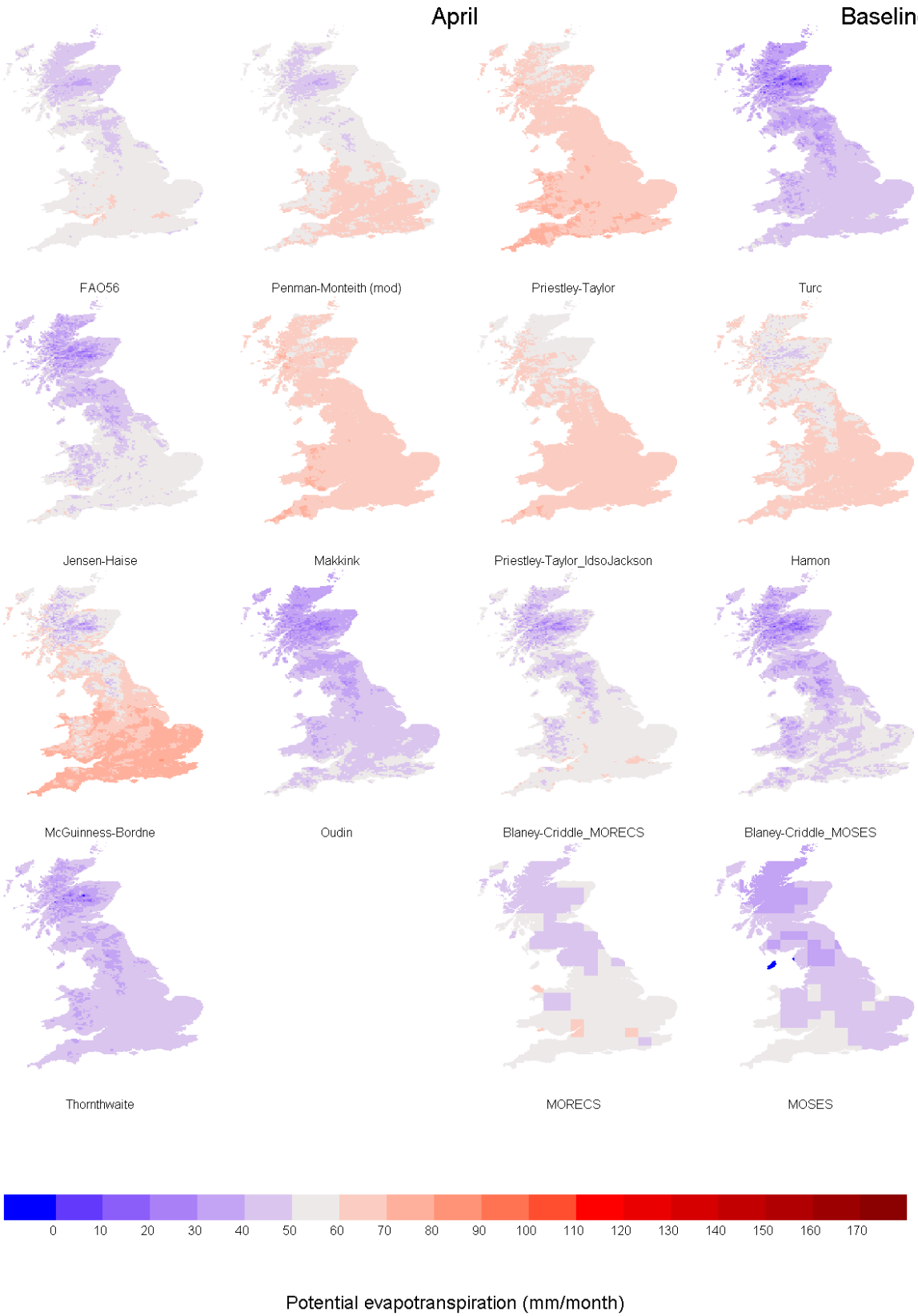

Figure 23: April mean. Potential evapotranspiration derived using HadRM3-afgcx climate data for the baseline period 1961-1990 using 13 PE equations and reference MORECS and offline MOSES PE. Radiation is derived from Shuttleworth (1993) equations

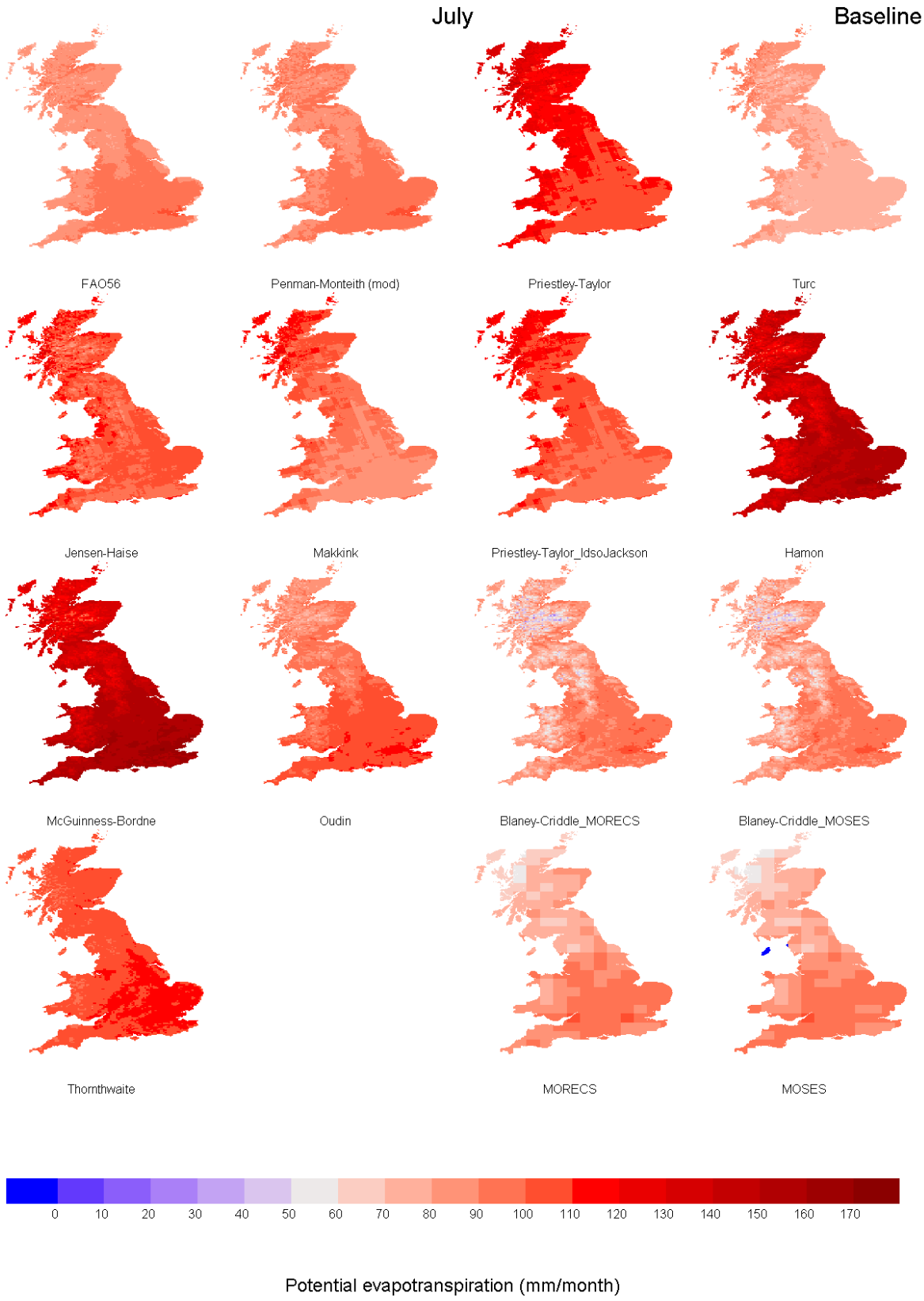

Figure 24: July mean. Potential evapotranspiration derived using HadRM3-afgcx climate data for the baseline period 1961-1990 using 13 PE equations and reference MORECS and offline MOSES PE. Radiation is derived from Shuttleworth (1993) equations

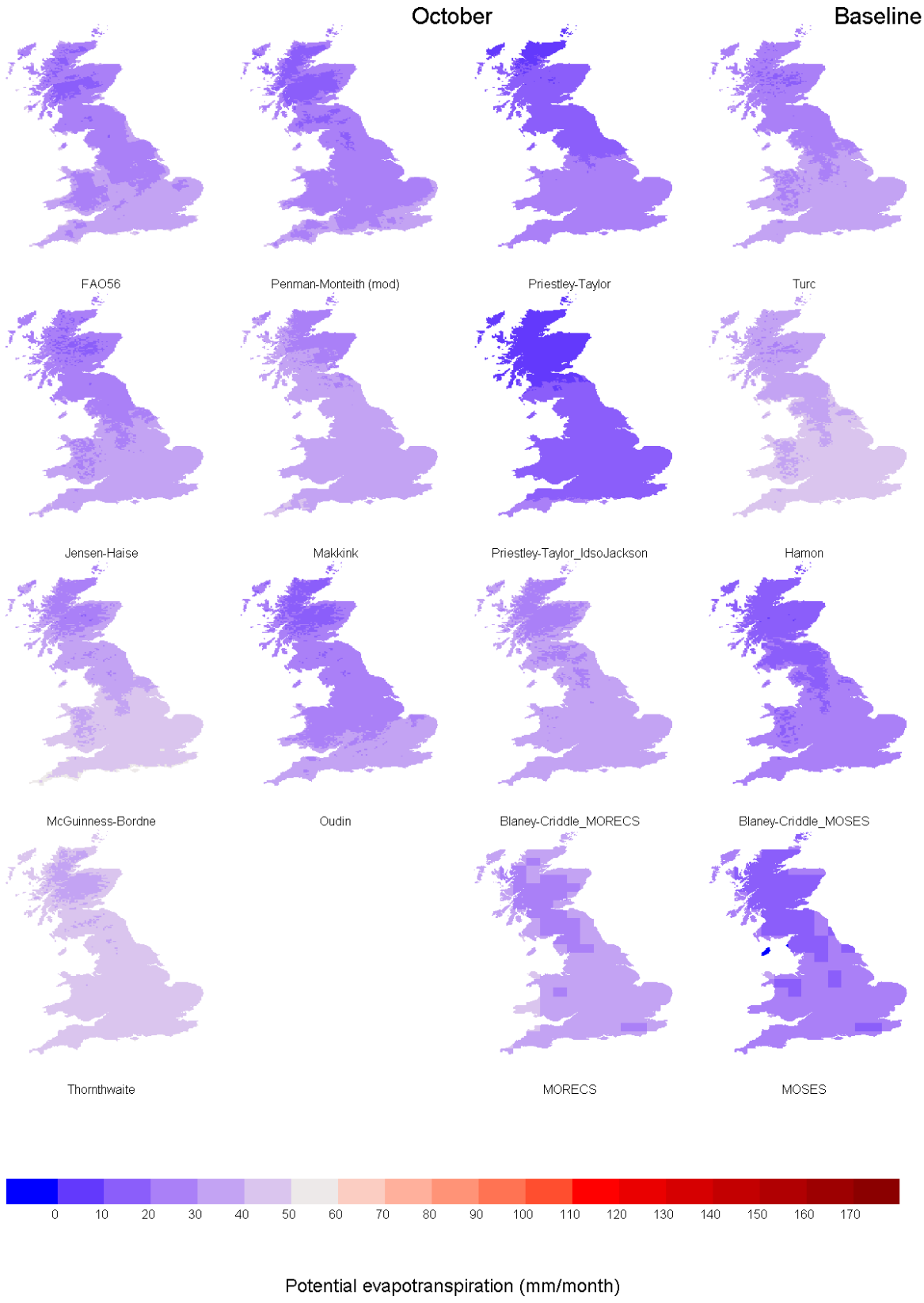

Figure 25: October mean. Potential evapotranspiration derived using HadRM3-afgcx climate data for the baseline period 1961-1990 using 13 PE equations and reference MORECS and offline MOSES PE. Radiation is derived from Shuttleworth (1993) equations

VI. 4 Reproduction of the spatial distribution of PE across GB using RCM radiation

Within HadRM3-PPE, net short and long-wave radiation are calculated as they are important energy components of the climate system. This section evaluates whether using direct RCM radiation improves PE estimates over deriving net radiation indirectly from other climate variables using the Shuttleworth (1993) equations (Section III. 4. 22.). This is because the UKCP09 probabilistic sample does not provide changes in short and long-wave radiation which are consistent with changes in precipitation and temperature.

For each equation, mean monthly PE was estimated using long-term RCM mean monthly climate variables as input data and compared with MORECS and offline MOSES for the four months typical of winter [January], spring [April], summer [July] and autumn [October]. Radiation (short and long wave) was either taken directly from afgcx or derived from Shuttleworth (1993) equations.

For the combined equations and Priestley Taylor, direct use of afcgx radiation systematically overestimates PE for all months over most of England and Wales in April (Figure 26) and July (Figure 27) compared to when using the radiation estimate from Shuttleworth (1993) equations. In January (Figure 26) and October (Figure 27) the pattern is reversed. In July, FAO-56 and Penman-Monteith (mod) reproduce well MORECS PE in Scotland when using RCM radiation, as opposed to a slight overestimation when not. This is, however, the only area where the direct use of RCM-radiation improves the estimate of PE. It is thus suggested not to use directly HadRM3-PPE radiation in this project.

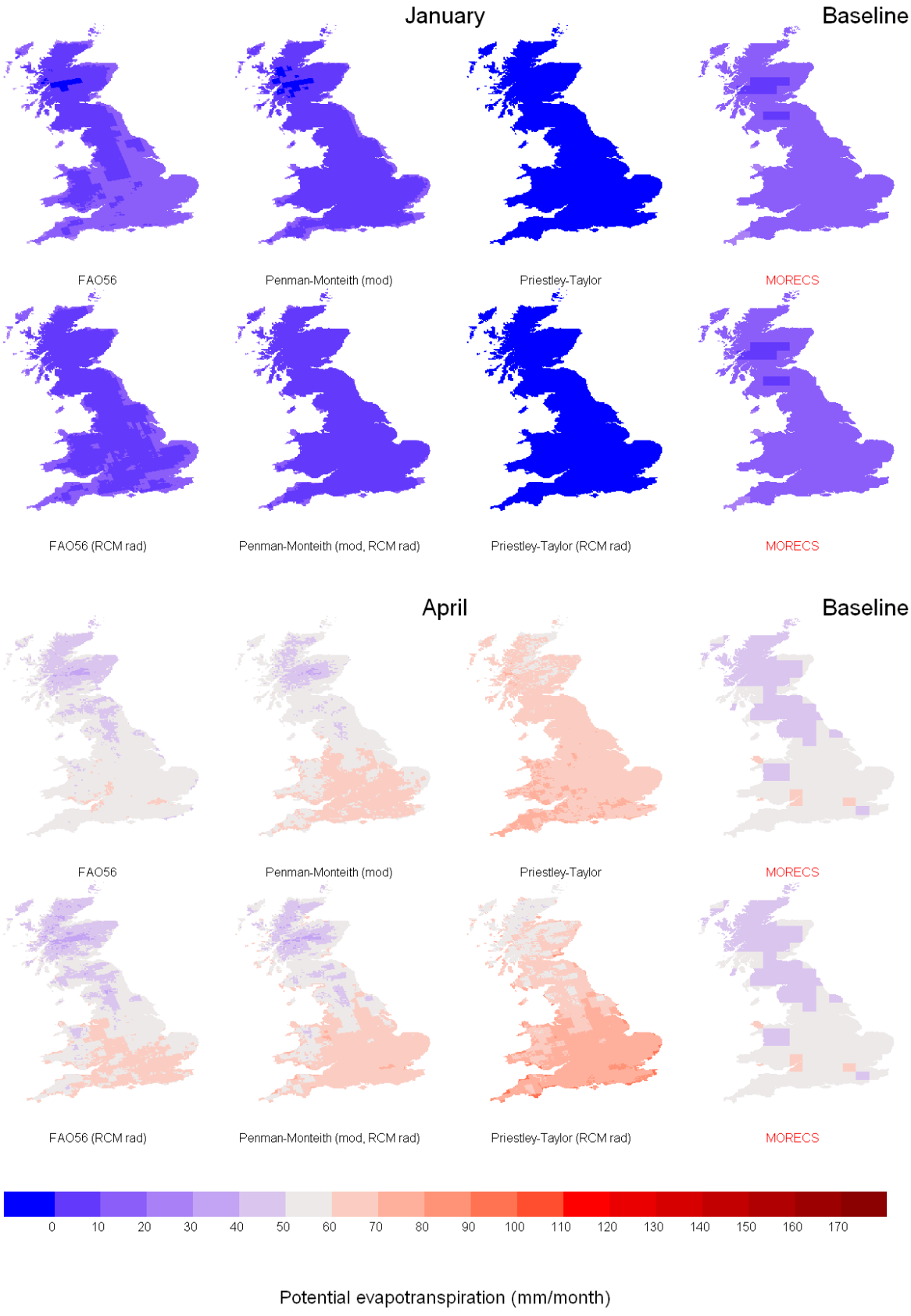

Figure 26: January (top two rows) and April (bottom two rows) mean. Potential evapotranspiration derived using HadRM3-afgcx climate data for the baseline period 1961-1990 using combined methods with (bottom) and without (top) RCM net Radiation estimates. MORECS PE is given for reference

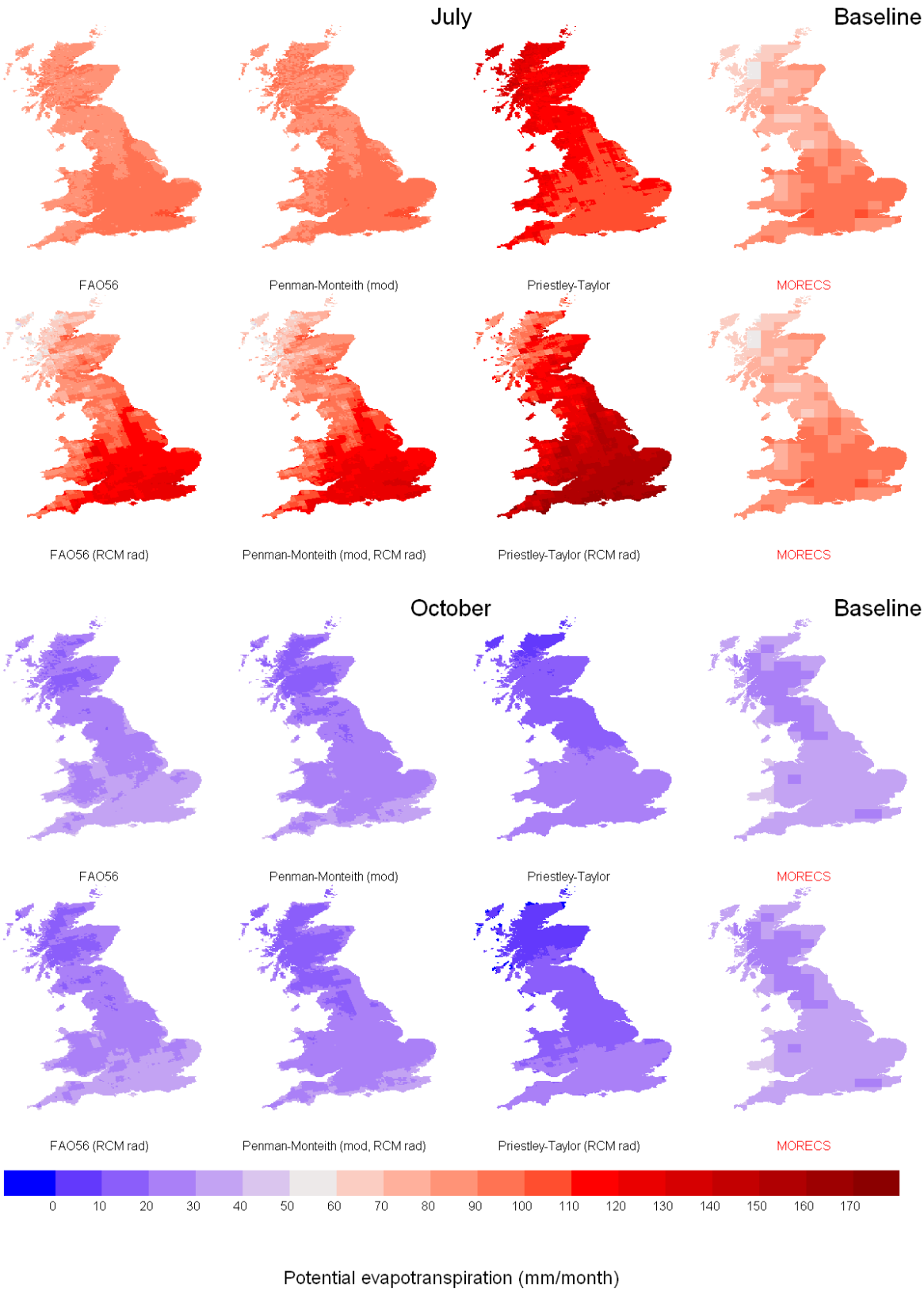

Figure 27: July (top two rows) and October (bottom two rows) mean. Potential evapotranspiration derived using HadRM3-afgcx climate data for the baseline period 1961-1990 using combined methods with (bottom) and without (top) RCM net Radiation estimates. MORECS PE is given for reference

Section VII Estimation of future change factors using different PE methods

VII. 1 Methodological framework

While the identification of the PE method which gives the best estimate of PE using RCM climate data for a baseline period is the main aim of this study, it is also important to quantify the impact of using different PE equations when estimating future PE change factors. This is particularly important as it could have consequences on changes in river flow estimations, as suggested by Kay and Davies (2008). In particular, temperature methods use temperature as the main potential source of energy for PE, neglecting other energy factors such as radiation and wind speed, and limiting factors such as humidity and vapour pressure. While such simplifications have often proved satisfactory for estimate of irrigation needs of crops, it is possible that their use in climate change study, where significant temperature rise is systematically projected, might lead to an overestimation of PE changes as changes in other factors that could compensate for warming are not accounted for.

This section aims to assess the implication of use of simplified PE methods compared to more complex ones in the quantification of changes in PE over Great Britain. Maps of changes in PE calculated as the percentage difference between future (2040-2069 or 2050s) and baseline (1961-1990) estimates of mean monthly PE using 13 PE methods are given in Section Table 4.

VII. 2 Results

For each equation, relative changes in mean monthly PE (PE change factors) were estimated using long-term RCM mean monthly climate variables as input data representative of the 2040-2069 (future) and 1961-1990 (baseline) periods for the four months typical of winter [January], spring [April], summer [July] and autumn [October] and presented as maps in Figure 28 to Figure 31. Radiation (short and long wave) was derived from Shuttleworth (1993) equations (Section III. 4. 22.).

Because of the very small absolute vales of PE in January, and thus associated large change factors, results for winter are not discussed. Apart from three methods (the two versions of Priestley Taylor and Makkink) suggesting a decrease in PE in April and in some parts of Wales, southeast England and Scottish highlands in July (in October only Priestley-Taylor-IdsoJackson suggests a PE decrease), all PE methods suggest an increase in PE by 2050. However, the magnitude and spatial pattern of this increase strongly varies by season and method. The largest discrepancies in PE change factors occur in July, where both BC methods suggest an increase of PE greater than 20%, while increases between 10 and 20% are suggested over the whole of Great Britain by Hamon, over Scotland and northern England by McGuinness-Bordne and Oudin, over the extreme north by Jensen-Haise, over the Midlands by FAO56 and Penman Monteith (mod), over southern England by FAO56, Penman Monteith (mod), McGuinness-Bordne, Oudin and to the extreme southeast by Thornthwaite. In April and October, changes are more spatially uniform for individual methods, but generally still range between 0 and 20%. Temperature methods seem to generally suggest larger increases than given by the combined and radiation methods except Thornthwaite (generally changes of same or lower magnitude) and Hamon in April. Note, however, that apart from BC methods in July, changes in the Midlands and southern England are of the same magnitude when estimated by combined and temperature methods. Changes in radiation methods are generally smaller than any other method. Note that these results contradict earlier work by Ekström et al. (2007) who found that FAO-56 method resulted in PE changes up to 4 times greater than BC methods by 2080s for the Northwest England, also using HadRM3. Note than unlike Ekström et al. (2007) who used minimum and maximum temperature to calculate the slope of vapour pressure /temperature

curve, only bias-corrected average temperature was used here. The strong intensification of the hydrological cycle by HadAM3H/HadRM3H hypothesised by Ekström et al. (2007) as the cause of this very large resulting signal in FAO-56 derived PE changes is less marked in the British Isles compared to the rest of Europe when looking at average temperatures which could be the reason why it does not impact much GB PE estimates as found in this study.

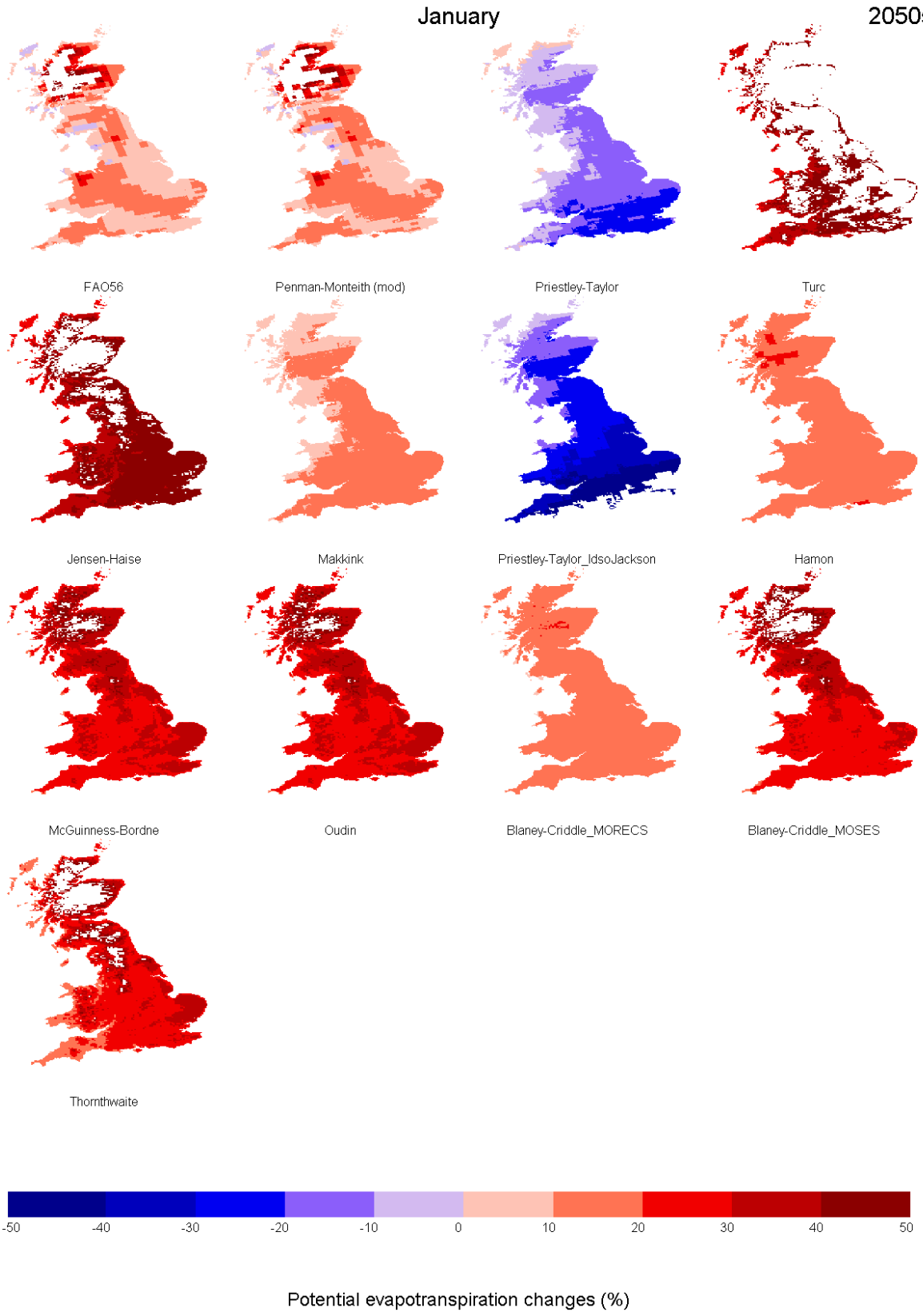

Figure 28: Change factors for the 2050s for January PE estimated from 13 methods. Radiation is estimated from climate variables. Note white areas outside the key range (increase in PE greater than 50%)

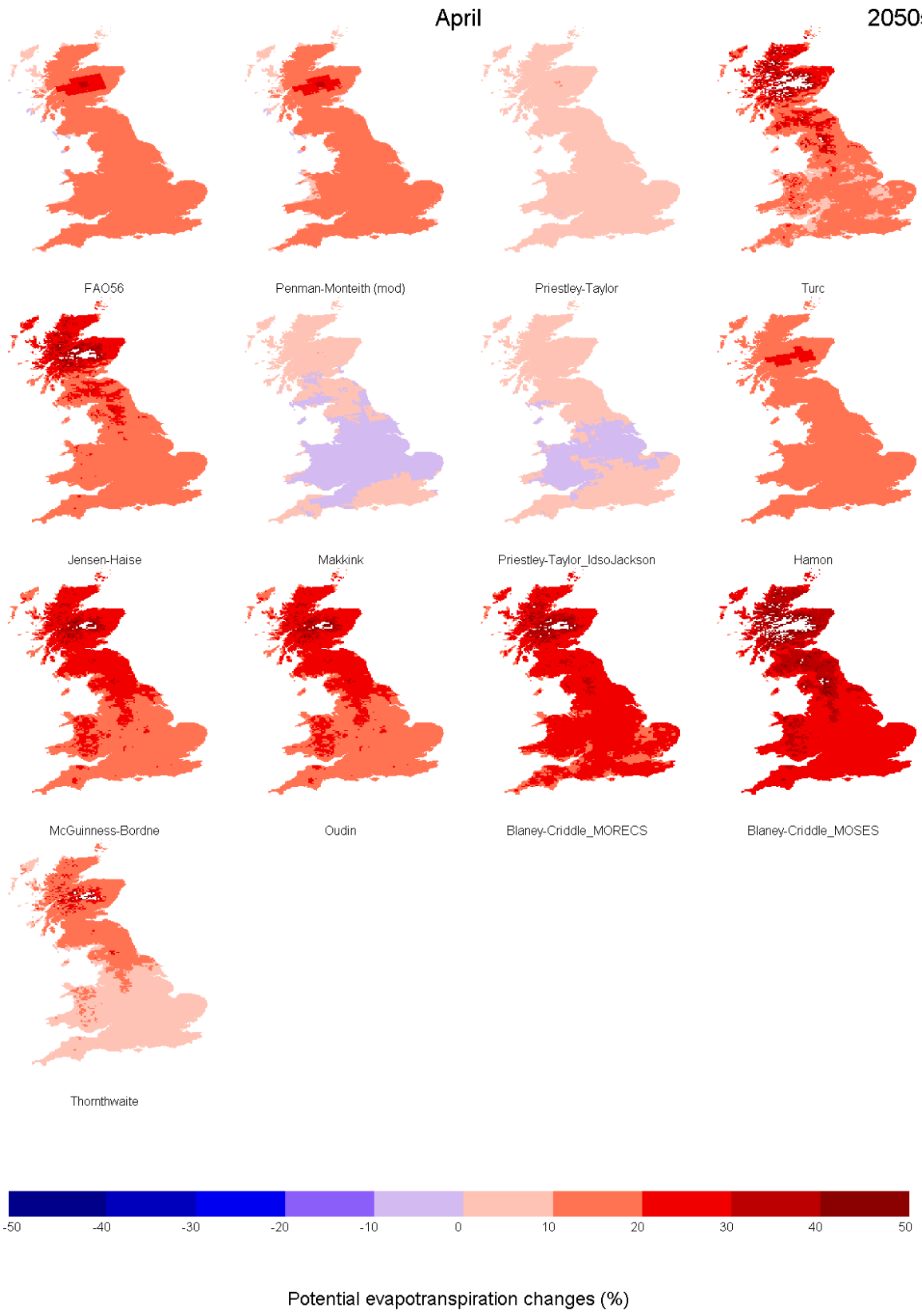

Figure 29: Change factors for the 2050s for April PE estimated from 13 methods. Radiation is estimated from climate variables

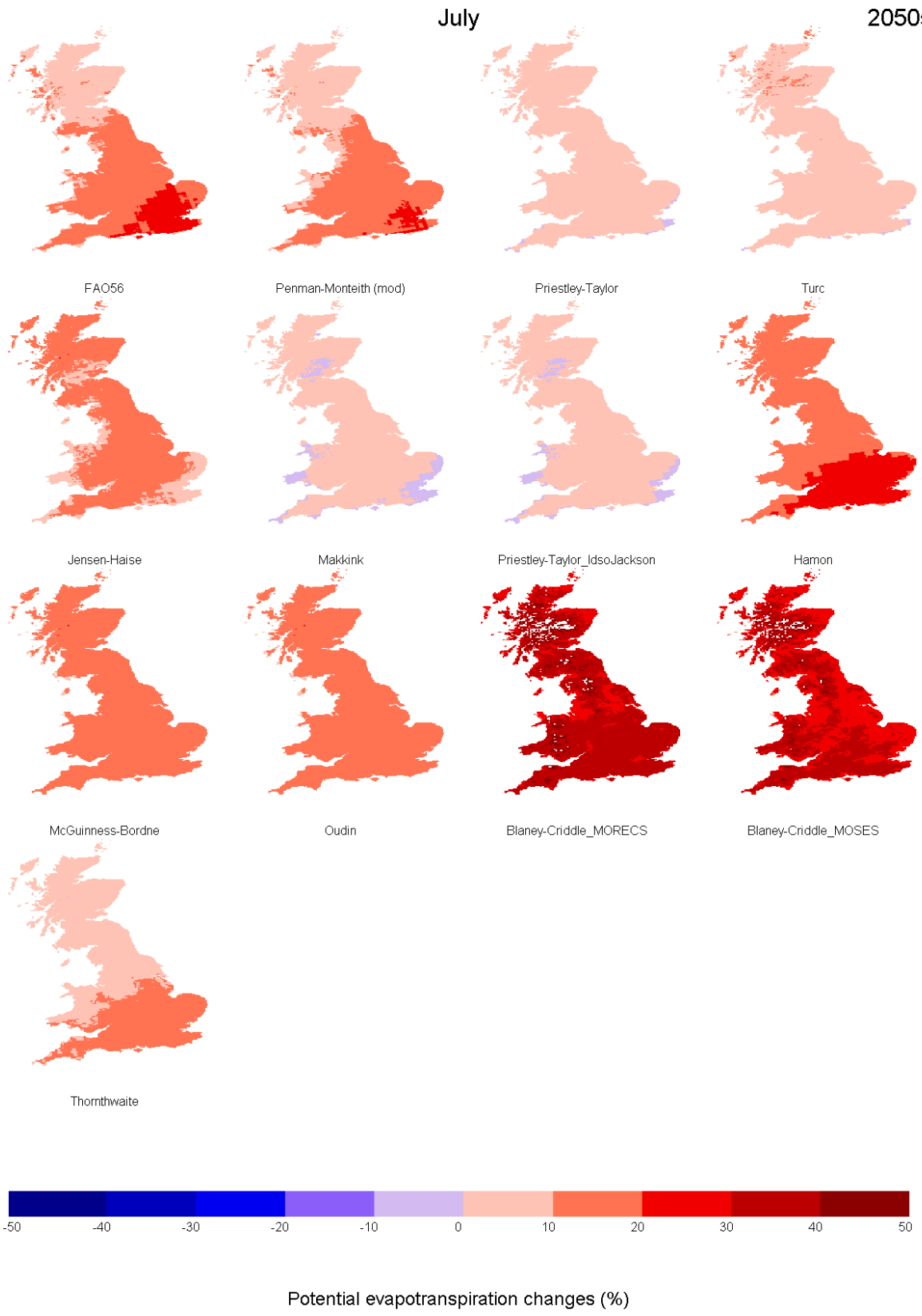

Figure 30: Change factors for the 2050s for July PE estimated from 13 methods. Radiation is estimated from climate variables

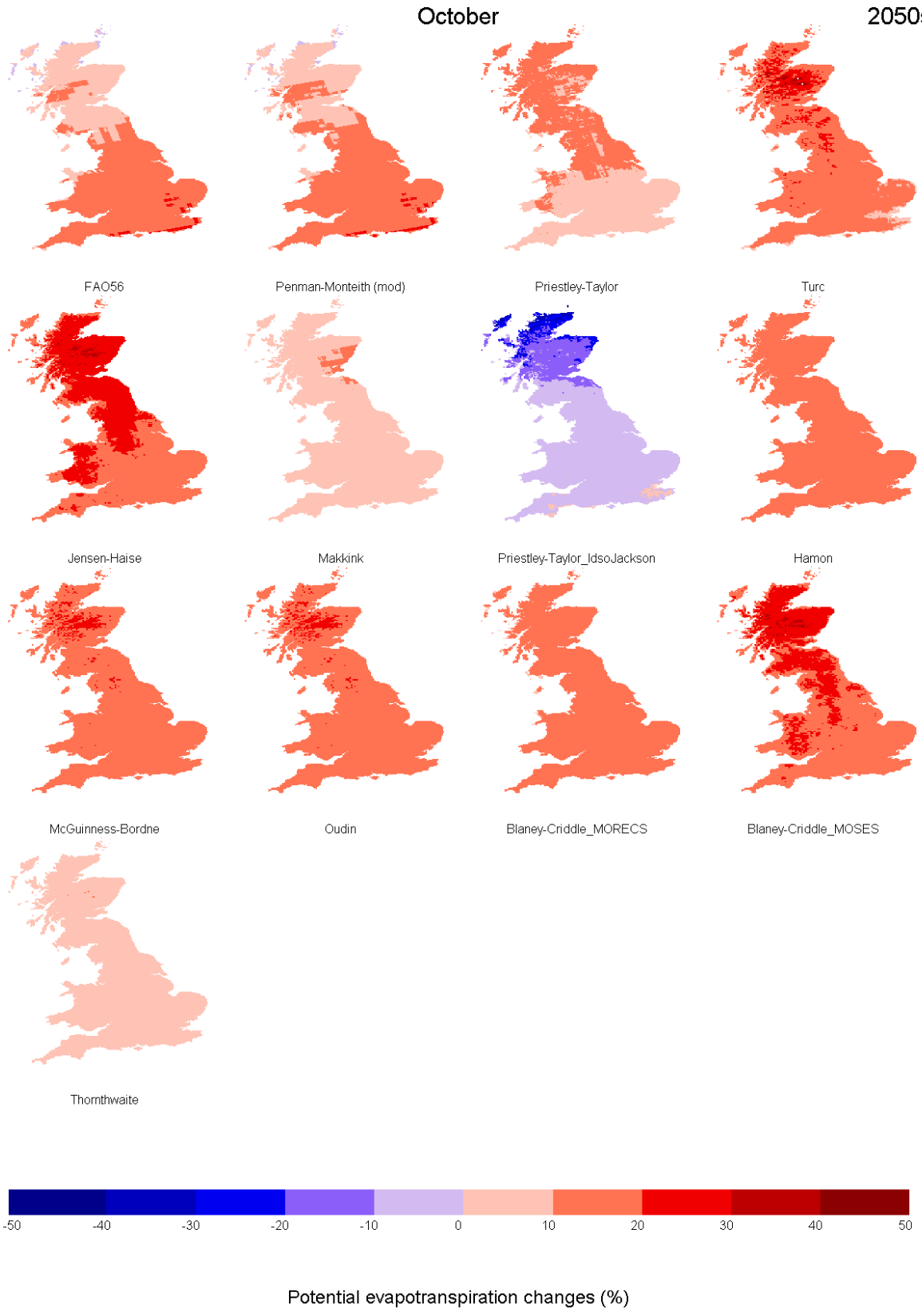

Figure 31: Change factors for the 2050s for October PE estimated from 13 methods. Radiation is estimated from climate variables

Section VIII Conclusions and recommendations

In this section, MORECS as been used as the reference PE in Great Britian.

VIII. 1 What are the acceptable PE methods using observed variables?

Comparison of spatial distribution of PE for average periods (1961-1990) and extreme years (dry: 1976; cool: 1985) showed that:

- Combined methods agree best with MORECS PE
- Temperature methods tend to overestimate MORECS, particularly in the summer, except Blaney Criddle
- Radiation methods agree better than temperature methods for the extreme years

VIII. 2 What are the acceptable PE methods minimising errors in river flows?

When comparing mean monthly observed and modelled flows for eight contrasting catchments of Great Britain:

- Best combined method: FAO-56
- Best radiation methods: Makkink and Jensen-Haise
- Best temperature methods: Blaney Criddle-MORECS and Oudin
- Best method across all catchments: FAO-56

VIII. 3 What are the acceptable PE methods using RCM variables?

Comparison of spatial distribution of mean monthly PE using RCM climate data showed that:

- Direct use of RCM radiation (net long and short wave) does not improve PE estimation
- Blaney Criddle-MORECS agrees best overall for most areas and seasons, but shows an unrealistic PE gradient in the summer (large underestimation of PE in uplands);
- FAO-56 reproduces reasonably well the PE spatial pattern, but tends to overestimate Scottish PE in the summer and underestimate PE in the midlands in autumn (low spatial variation in the monthly estimates)
- The other models do not provide satisfactory spatial distribution of PE throughout the year

VIII. 4 Change factors for the 2050s compared to baseline using RCM variables

- No consistency in magnitude of changes between PE methods
- Temperature methods generally have the highest changes (greater than 10%) (expect Thornthwaite)
- Combined methods have changes between 0 and 20%
- Radiation methods have the lowest changes (less than 10% increase) and sometimes suggest decrease in PE
- Blaney Criddle shows very large increases in July PE (over 20%) not reproduced by any other method

VIII. 5 Recommendations

Taking all results into consideration, FAO-56 is suggested as the most suitable PE method to use in this project as:

- The empirical formulae of the Blaney Criddle method have been calibrated over the 1961-1990 period, and could not be assessed in any other period
- The very large changes in summer PE obtained when using Blaney Criddle are not reproduced by any other method, and could be an overestimation due to a too large role of temperature in the estimation of PE
- FAO-56 (using climate-derived radiation) does reproduce reasonably well the spatial and temporal distribution of PE across Great Britain despite some slight overestimation in summer in the Scotland when using both observed and RCM-derived climate variables
- The use of bias-correction for temperature, possibly resulting in some slight inconsistency with other climate variables, does not seem to significantly compromise the ability of FAO-56 to reproduce PE in Great Britain [Note the use of HadRM3 temperature without bias-correction was not tested]
- Note that for the probabilistic estimation of PE changes wind speed in FAO-56 be assumed unchanged in the future as no change in wind speed is available that is consistent with other climate variables

Section IX References

Allen, R. G., Pereira, L. S., Raes, D. & Smith, M. 1998. FAO irrigation and drainage paper 56 - Crop evapotranspiration - Guidelines for computing crop water requirements. Rome: Food and Agriculture Organisation of the United Nations.

Allen, R. G., Smith, M., Pereira, L. S. & Perrier, A. 1994. An update for the calculation of reference evapotranspiration. *ICID Bulletin 1944.* ICID Bulletin.

Blaney, H. F. & Criddle, W. D. 1950. Determining water requirements in irrigated areas from climatological and irrigation data. *Technical paper N 96, US Department of Agriculture Soil Conservation Service.* Washington, USA.

Brunt, D. 1934. *Physical and dynamical meteorology,* Cambridge, University press.

Cox, P. M., Betts, R. A., Bunton, C. B., Essery, R. L. H., Rowntree, P. R. & Smith, J. 1999. The impact of new land surface physics on the GCM simulation of climate and climate sensitivity. Climate Dynamics*,* **15,** 183-203, doi.

Ekström, M., Jones, P. D., Fowler, H. J., Lenderink, G., Buishand, T. A. & Conway, D. 2007. Regional climate model data used within the SWURVE project – 1: projected changes in seasonal patterns and estimation of PET. Hydrology and Earth System Sciences*,* **11,** 1069-1083, doi: 10.5194/hess-11-1069-2007.

Hamon, W. R. 1961. Estimating potential evapotranspiration. Journal of the Hydraulics Division - Proceesings of the American Society of Civil Engineers*,* **87,** 107-120, doi.

Hough, M. 2003. An historical comparison between the Met Office Surface Exchange Scheme-Probability Distributed Model (MOSES-PDM) and the Met Office Rainfall and Evaporation Calculation System (MORECS). *Report for the Environment Agency and the Met. Office.* Bracnkell: Met Office.

Jacobs, A. F. G., Heusinkveld, B. G. & Holtslag, A. a. M. 2009. Eighty years of meteorological observations at Wageningen, the Netherlands: precipitation and evapotranspiration. International Journal of Climatology*,* **30,** 1315-1321, doi: DOI:10.1002/joc.1957.

Jensen, M. E., Burman, R. D. & Allen, R. G. (eds.) 1990. *Evapotranspiration and irrigation water requirements,* New York: American Society of Civil Engineers.

Kay, A. L., Bell, V. A., Moore, R. J. & Jones, R. G. 2003. Estimation of UK flood frequencies using RCM rainfall: an initial investigation. *Met Office Annex 15a subcontract report 1.* Wallingford: CEH.

Kay, A. L. & Davies, H. N. 2008. Calculating potential evaporation from climate model data: a source of uncertainty for hydrological climate change impacts. Journal of Hydrology*,* **358,** 221-239, doi.

Linsley, R. K. J., Kohler, M. A. & Paulhus, J. L. H. 1988. *Hydrology for engineers - SI metric edition,* London, McGraw-Hill Book Company.

Murphy, J. M., Sexton, D. M. H., Jenkins, G. J., Booth, B. B. B., Brown, C. C., Clark, R. T., Collins, M., Harris, G. R., Kendon, E. J., Betts, R. A., Brown, S. J., Humphrey, K. A., Mccarthy, M. P., Mcdonald, R. E., Stephens, A., Wallace, C., Warren, R., Wilby, R. &

Wood, R. A. 2009. UK Climate Projections Science Report: Climate Change Projections. Exeter, UK: Met Office Hadley Centre.

Oudin, L., Hervieu, F., Michel, C., Perrin, C., Andreassian, V., Anctil, F. & Loumagne, C. 2005. Which potential evapotranspiration input for a lumped rainfall-runoff model?: Part 2--Towards a simple and efficient potential evapotranspiration model for rainfall-runoff modelling. Journal of Hydrology, **303,** 290-306, doi.

Priestley, C. H. B. & Taylor, R. J. 1972. On the assessment of surface heat flux and evaporation using large-scale parameters. Monthly Weather Review, **100,** 81-92, doi.

Shuttleworth, W. J. 1993. Evaporation. *In:* MAIDMENT, D. R. (ed.) *Handbook of hydrology.* McGraw-Hill, Inc.

Thompson, N., Barrie, I. A. & Ayles, M. 1982. The Meteorological Office Rainfall and Evaporation Calculation System: MORECS (July 1981). *Hydrological Memorandum N 45.* Bracknell, UK: Met. Office.

Thornthwaite, C. W. 1948. An approach toward a rational classification of climate. Geographical Review, **38,** 55-94, doi.

Turc, L. 1961. Evaluation des besoins en eau d'irrigation, evapotranspiration potentielle. Ann. Agron., **12,** 13-49, doi.

Xu, C. Y. & Singh, V. P. 2001. Evaluation and generalization of temperature-based methods for calculating evaporation. Hydrological Processes, **15,** 305-319, doi.